Zoologischer Anzeiger
November 2022, Volume 301 Pages 179-195
https://doi.org/10.1016/j.jcz.2022.10.008
https://archimer.ifremer.fr/doc/00801/91300/

Two new species of the *Echinoderes coulli*-group (Kinorhyncha: Cyclorhagida: Echinoderidae) from a low human-impacted mangrove swamp in French Guiana (western Atlantic Ocean)

Cepeda Gomez Diego [1, *], Gayet Nicolas [1], Spedicato Adriana [2], Michaud Emma [2], Zeppilli Daniela [1]

[1] Deep-Sea Laboratory (LEP), French Institute for Ocean Science (IFREMER), ZI de La Pointe du Diable, CS 10070, 29280, Plouzané, France
[2] Univ. Brest, CNRS, IRD, Ifremer, LEMAR, F-29280, Plouzané, France

* Corresponding author : Diego Cepeda Gomez, email address : dcepedag@ifremer.fr

Abstract :

The Echinoderes coulli-group is characterized by the presence of an enlarged nephridiopore composed of two regions apparently related to increase the osmoregulation efficiency. Representatives of this group are often intertidal species living in habitats with daily salinity changes, including mangroves. In the present study, two new species potentially belonging to this group are described from a lowly polluted mangrove in French Guiana (western Atlantic Ocean). Echinoderes angelae sp. nov. possesses spines in middorsal position on segment 4 and sublateral position on segments 6–7, plus tubes in lateroventral position on segments 5 and 8 and in laterodorsal position on segment 10. Besides, this species has modified type 2 glandular cell outlets throughout different positions on segments 2, 4–8 and 10 and large sensory spots on segment 1 with a transversal row of conspicuously elongated hairs at the posterior part of the papillae area. Echinoderes guianensis sp. nov. has spines in middorsal position on segment 4, lateroventral position on segment 6 and sublateral position on segment 7, plus tubes in lateroventral position on segment 5 and laterodorsal position on segment 10. Also, it lacks modified type 2 glandular cell outlets and large sensory spots with a posterior, transversal row of elongated hairs. These diagnostic features allow the distinction of the new species from the remaining congeners of the E. coulli-group. In addition, the presence of epibionts in some of the examined specimens is discussed.

Keywords : Kinorhynchs, Mud dragons, Mangrove forest, Taxonomy, Human impact, Contamination

1. Introduction

Mangroves are among the most remarkable, tropical and subtropical, marine, intertidal ecosystems due to their economic and ecological relevance (Pillai & Harilal 2018). These forests are hold by marine alluvium sediment rich in organic matter and anaerobic, sulphur-reducing bacteria activity (Hossain & Nuruddin 2016). These features make mangroves a challenging habitat for organisms that live in the sediment, including the meiofauna (Edgar 1990; Sasekumar & Chong 1998; Kathiresan & Bingham, 2001).

Although studies on mangrove meiofauna are relatively abundant for its key role within benthic communities (e.g. Castel 1992; Olafsson et al. 2000; Mokievsky et al. 2011; Sahoo et al. 2013; Della Patrona et al. 2016; Michelet et al. 2021), some meiofauna components are often neglected due to the lack of taxonomic expertise or low-abundance levels, which is the case of the phylum Kinorhyncha. Kinorhynchs can be among the top three dominant groups in riverine and fringe mangroves, with values of ca. 39–160 ind/10cm^2 (Gomes et al. 2002; Ostmann et al. 2012; Annapurna et al. 2015; Cepeda et al. 2022). Many of the known kinorhynch species inhabiting mangrove habitats belong to the *Echinoderes coulli*-group, characterized by the possession of an enlarged nephridiopore to cope with strong salinity fluctuations (Cepeda et al. 2022).

In order to increase our knowledge about the taxonomic composition of the mangrove meiofaunal species in general, and the kinorhynch species in particular, two new species of *Echinoderes* Claparède, 1863 are formally described from a low human-impacted mangrove swamp in French Guiana (western Atlantic Ocean), which putatively belong to the *E. coulli*-group.

2. Material and methods

Kinorhynchs of the present study come from sediment samples previously sorted and analysed in Michelet et al. (2021). The study area was represented by adult mangroves throughout the polyhaline zone in the Cayenne Estuary, French Guiana (western Atlantic Ocean). Three sampling stations were selected: one along the Crique Fouillée tributary (04°54′53.208″ N, 52°20′15.9324″ W), one near the confluence of the Cayenne and Montsinéry Rivers (04°53′49.2288″ N, 52°22′27.714″ W), and one located 14km upstream of the Cayenne River (04°51′31.9716″ N, 52°23′59.5248″ W) (Fig. 1). The mangrove forest was mainly composed

of *Avicennia germinans* (L.) with some intercalated patches of *Laguncularia racemosa* (C.F. Gaertn, 1807) and *Rhizophora* sp. As already described by Michelet et al. (2021) and Fiard et al. (2022), this area was influenced by low concentrations of pollutants below toxicity guidelines.

Sediment samples were collected by hand using Plexiglas® cores of 10.4cm internal diameter and 20cm height during low tide. Each sediment column was divided into three depth layers: first layer, 0–2 cm depth; second layer, 2–10 cm depth; third layer, 10–16 cm depth. Subsamples of 1.77 cm^2 were taken at the three layers of each core for taxonomic purposes, consequently fixed in 4% formalin buffered with sodium bicarbonate.

Meiofauna was extracted from sediment by LUDOX® colloidal silica centrifugation (Heip et al. 1985). Kinorhynchs were separated from the remaining organisms under a stereomicroscope and preserved in 70% ethanol. For light microscopy (LM), specimens were gradually passed to glycerine and mounted on glass slides with Fluoromount G®. A Leica DM2500® LED compound microscope equipped with differential interference contrast (DIC) was used. For scanning electron microscopy (SEM), specimens were passed through a graded series of ethanol until 100% ethanol, critical point dried, mounted on stubs, coated with gold (10–20 nm thickness) and studied in a Thermofisher™ Quanta 200 microscope at 5.00kV and 10.5 mm work distance.

Line art drawings of the new species and micrograph plates composition were prepared using Adobe® Photoshop and Illustrator CS6 software. Type and additional material for LM was deposited at the Muséum Natural d'Histoire Naturelle (MNHN), France.

3. Results

Taxonomic account

Class **Cyclorhagida** (Zelinka, 1896) Herranz et al., 2022

Family **Echinoderidae** Carus, 1885

Genus ***Echinoderes*** Claparède, 1863

3.1 ***Echinoderes angelae*** **sp. nov.**

urn:lsid:zoobank.org:act:482926BC-199C-4168-BB67-92E21CB0ACF5

(Figs. 2–8, Tables 1–2)

3.1.1 Material examined

Holotype, adult female, collected in November 2017 at the confluence of the Cayenne and Montsinéry Rivers, French Guiana (western Atlantic Ocean): 04°53′49.2288″ N, 52°22′27.714″ W at the intertidal zone in mud; mounted in Fluoromount G®, deposited at MNHN under catalogue number: 655Ma. Paratypes, three adult males and five adult females, same collecting data as holotype; mounted in Fluoromount G®, deposited at MNHN under catalogue numbers: 656Ma–663Ma. Additional material, 29 adult males, 23 adult females, 3 adults of unknown sex, 83 juveniles and 12 exuvia, some of them with same collecting data as type material, mounted in Fluoromount G®, others collected in November 2017 ca. 14km upstream of the Cayenne River, French Guiana (western Atlantic Ocean): 04°51′31.9716″ N, 52°23′59.5248″ W at the intertidal zone in mud; mounted in Fluoromount G®, deposited at MNHN under catalogue numbers: 666Ma–815Ma; seven adult males, eight adult females, three adults of unknown sex and eight juveniles, same collecting data as type and remaining additional material, mounted for SEM, deposited at IFREMER.

3.1.2 Diagnosis

Echinoderes with short, poorly sclerotized, weakly articulated spines in middorsal position on segment 4 and sublateral position on segments 6–7. Tubes in lateroventral position on segment 5, lateral accessory position on segment 8 and laterodorsal position on segment 10. Modified type 2 glandular cell outlets in subdorsal position on segments 2 and 5–8, laterodorsal position on segments 2, 4 and 10, midlateral position on segments 2, 6 and 8, and lateroventral position on segments 7–8. Large, rounded sensory spots on segment 1 with a transversal row of conspicuously elongated hairs at the posterior edge of the papillae area. Enlarged, oval sieve plate in sublateral position on segment 9, consisting of an anterior, slightly convex region with numerous pores and a posterior, slightly concave area with a single, central pore.

3.1.3 Etymology

The species is dedicated to Ángela Cepeda Gómez, sister of the first author, for all these years of unconditional support.

3.1.4 Description

See Table 1 for measurements of selected morphological features and body dimensions, and Table 2 for summary of spine, tube, nephridiopore, glandular cell outlet and sensory spot locations.

Despite the high number of studied specimens, only a few had the head everted, hence only some data of the morphology and appendage arrangement are provided. Ring 00 of mouth cone with nine outer oral styles alternating in size between slightly larger and smaller ones. Outer oral styles composed of two jointed subunits: a rectangular, basal sheath with distal fringe and a triangular, hooked, distally pointed end-piece. Outer oral styles located anterior to each introvert sector, except in the middorsal sector 6 where a style is missing (Figs. 2; 4B).

Introvert with seven concentric rings of spinoscalids (one ring of primary spinoscalids and six rings of regular-sized spinoscalids) and 10 longitudinal sectors defined by the arrangement of the primary spinoscalids. Ring 01 with 10 primary spinoscalids, larger than remaining scalids, composed of a basal sheath and a distal, elongated, flexible end-piece. Ring 02 with 10 spinoscalids, arranged as one medially in each sector; spinoscalids on this and following rings are morphologically similar to the primary spinoscalids but smaller. Ring 03 with 20 spinoscalids, arranged as two in each sector. Ring 04 with 10 spinoscalids, arranged as one medially in each sector. Ring 05 with 20 spinoscalids, arranged as two in each sector. Ring 06 with five spinoscalids, arranged as one medially in each odd-numbered sector. Ring 07 with an unknown number of smaller spinoscalids, as only those of sectors 1, 3 and 4 could be observed (sectors 1 and 3 with three spinoscalids, sector 4 with two leaving space for the corresponding trichoscalid and its plate); sectors 9 and 8 are likely similar to sectors 3 and 4 in this arrangement due to the typical radial symmetry of the kinorhynch introvert. Scalid arrangement identical in all sectors from rings 02–05, with one unpaired scalid in ring 02 followed by a quincunx in rings 03–05; in sectors 1 (and likely 9), ring 06 with an unpaired scalid followed by three smaller scalids in ring 07; in sectors 4 (and likely 8), ring 06 without scalids followed by two smaller scalids in ring 07 leaving space for the corresponding trichoscalid and its plate; rings 06–07 unknown for remaining sectors. A fringed ring around the introvert at the level of rings 04–05, with tips more elongated in sectors where a spinoscalid is missing in ring 06 (Figs. 2; 6B-C).

Neck with 16 trapezoidal placids, wider at the base, closely adjacent each other, with distinct joint between the neck and first trunk segment. Midventral placid widest (ca. 10–11µm at base), remaining ones slightly narrower (ca. 6–8µm at base). A ring of six short, superficially

haired trichoscalids associated with the placids, attached to quadrangular trichoscalid plates in sectors 2, 4, 5, 7, 8 and 10 (Figs. 2; 3A-B; 4C-D; 6A-D).

Trunk fusiform, heart-shaped in cross-section, composed of 11 segments. Segments 1–2 closed, ring-like cuticular plates; remaining ones with one tergal and two sternal cuticular plates (Figs. 3A-D; 4A; 5A-F; 6A; 7B). Maximum sternal width at segment 8, relatively narrow compared to total trunk length (MSW8/TL average ratio = 19.6%). Cuticular hairs throughout segments 2–11 (absent on segment 1), acicular, non-bracteate, emerging from rounded to slightly oval perforation sites. Cuticular hairs arranged as 6–12 transversal, uninterrupted rows covering the cuticular surface of segments 2–3 (except in the ventromedial region where hairs are missing); as 6–16 transversal rows that become wavy at subdorsal and ventrolateral to ventromedial regions, interrupted by large, oval, muscular scars in laterodorsal position throughout segments 4–10; as 6–8 transversal, uninterrupted rows covering the cuticular surface of segment 11 (hairs of this segment conspicuously shorter) (Figs. 3A-D; 5A-F; 7B, D, F, H, L). Posterior segment margins straight, with serrated primary pectinate fringe (Fig. 3A-D); primary pectinate fringe of segment 1 with larger tips (Fig. 7B); segments 2 and 10 with posterior segment margin extended as a triangle in the ventrolateral to ventromedial region, with tips of primary pectinate fringe conspicuously shorter and tighter than those on other regions on the same segment (Figs. 3A-D; 7B, L); segments 3–9 with tips of primary pectinate fringes noticeable shorter and tighter in the ventromedial region than those on other regions on the same segment (Fig. 7B); segment 11 with elongated tips of primary pectinate fringe in middorsal to subdorsal and lateroventral to ventrolateral regions (Figs. 3A-D; 6F-G). Secondary pectinate fringes finely serrated (Fig. 7K).

Segment 1 with type 1 glandular cell outlets in middorsal and lateroventral positions (Figs. 3A-B; 5A). Large, rounded sensory spots in subdorsal, laterodorsal and ventromedial positions, the former two located near the anterior segment margin, the latter near the posterior segment edge; these sensory spots have a transversal row of conspicuously elongated hairs at the posterior edge of the papillae area (except in seven specimens mounted for SEM that lacked these hairs, see subsection *3.1.5 Notes on intraspecific variability*) (Figs. 3A-B; 5A; 7A).

Segment 2 with one pair of droplet-shaped sensory spots in middorsal and ventromedial positions, and two pairs in laterodorsal position (Figs. 3A-B; 5A); on this and following segments, these sensory spots usually have one or two central pores with emerging cilia (Fig. 7D). Modified type 2 glandular cell outlets in subdorsal, laterodorsal and midlateral positions

(Figs. 3B; 5A; 7D); on this and following segments, modified type 2 glandular cell outlets are minute, oval, glandular openings surrounded by a tuft of short cuticular extensions (Fig. 7C).

Segment 3 with type 1 glandular cell outlets in middorsal and ventromedial positions (Fig. 3A-B). Droplet-shaped sensory spots in subdorsal and midlateral positions (Figs. 3B; 7H).

Segment 4 with short (ca. 4–8µm length), poorly sclerotized, weakly articulated, acicular spine in middorsal position (Figs. 3B; 7G). Type 1 glandular cell outlets in subdorsal and ventromedial positions (Fig. 3A-B). Modified type 2 glandular cell outlets in laterodorsal position (Figs. 3B; 7C).

Segment 5 with tubes in lateroventral position (Figs. 3A; 5C). Type 1 glandular cell outlets in subdorsal and ventromedial positions (Fig. 3A-B). Modified type 2 glandular cell outlets in subdorsal position (Fig. 3B). Droplet-shaped sensory spots in subdorsal, midlateral and ventromedial positions; subdorsal sensory spots more lateral than subdorsal modified type 2 glandular cell outlets (Figs. 3A-B; 5B-C; 7B).

Segment 6 with short (ca. 4–6µm length), poorly sclerotized, weakly articulated, acicular spines in sublateral position (Figs. 3A; 5C). Type 1 glandular cell outlets in subdorsal and ventromedial positions (Fig. 3A-B). Modified type 2 glandular cell outlets in subdorsal and midlateral positions (Figs. 3B; 5B). Droplet-shaped sensory spots in subdorsal, midlateral and ventromedial positions; subdorsal sensory spots more mesial than subdorsal modified type 2 glandular cell outlets (Figs. 3A-B; 5B-C; 7B).

Segment 7 similar to segment 6 regarding spine, glandular cell outlet and sensory spot arrangement, but with modified type 2 glandular cell outlets in lateroventral instead of midlateral position and sensory spots in ventrolateral instead of ventromedial position (Figs. 3A-B; 5B, F; 7J).

Segment 8 with tubes in lateral accessory position (Figs. 3A; 5F; 7J). Type 1 glandular cell outlets in subdorsal and ventromedial positions (Fig. 3A-B). Modified type 2 glandular cell outlets in subdorsal, midlateral and lateroventral positions (Figs. 3A-B; 5D, F; 7F). Droplet-shaped sensory spots in subdorsal position (Figs. 3B; 5D; 7F).

Segment 9 with type 1 glandular cell outlets in subdorsal and ventromedial positions (Figs. 3A-B; 7K). One pair of droplet-shaped sensory spots in midlateral and ventrolateral positions, and two pairs in subdorsal position (Figs. 3A-B; 5D-E; 7F, M). Nephridiopores in sublateral position as enlarged sieve plate openings with an anterior, elongated, slightly convex

area with numerous pores and a posterior, slightly concave region with a single, central pore (Figs. 3A; 5E; 7E).

Segment 10 with tubes in laterodorsal position, larger in males (Figs. 3B, D; 4E; 7I). Two type 1 glandular cell outlets in middorsal position, longitudinally arranged; type 1 glandular cell outlets also in ventromedial position (Fig. 3A-B). Modified type 2 glandular cell outlets in laterodorsal position, anterior to the tubes (Fig. 3B). Droplet-shaped sensory spots in subdorsal and ventrolateral positions (Figs. 3A-D; 5E; 7L).

Segment 11 with relatively short lateral terminal spines (LTS:TL average ratio = 17.9%), distally pointed, with hollow central cavity, superficially covered by hairs (Figs. 3A-D; 4A, E-F, H-I; 6A, E-G). Males with three pairs of penile spines that emerge from laterodorsal position in the intersegmental joint with the preceding segment; penile spines tube-like, covered by hairs, abruptly tapering near their distal tips (Figs. 3D; 4E; 6F). Females with short (LTAS:LTS average ratio = 28.5%), distally frayed, covered by hairs, lateral terminal accessory spines, and oval, ventrolateral gonopores near the intersegmental joint with the preceding segment (Figs. 3A-B; 4F; 6G). Droplet-shaped sensory spots in subdorsal and ventromedial positions (Figs. 3A-D; 7L). Tergal extensions triangular, distally pointed, covered by hairs, distally elongated as hair-like extensions (Figs. 3A-D; 4F; 6E).

3.1.5 Notes on intraspecific variability

Echinoderes angelae sp. nov. shows certain degree of intraspecific variability not related to sex or sampling station. One of the most remarkable features of the species is the presence of three pairs of large sensory spots on segment 1 with a transversal row of conspicuously elongated hairs at the posterior edge of the papillae area (Figs. 3A-B; 5A; 7A). However, seven specimens mounted for SEM (four males and three females) showed these sensory spots without such kind of hairs (Fig. 7A). Neither juveniles of the species possess the elongated hairs, which suggests that the observed specimens could be pre-adults that did not develop the structures yet.

Shape and position of nephridiopores also showed variation among the studied specimens. This structure varies from completely oval or slightly triangular, located near the anterior margin of segment 9 without rows of hairs on top (ca. 70% of the examined specimens) to more buttonhole-shaped, posteriorly displaced having a few rows of hairs on top (ca. 30% of

the examined specimens) (Figs. 5E; 7E). These differences were observed in both LM and SEM specimens.

Segments 10 and 11 also showed conspicuous intraspecific variability regarding the length of the tergal extensions and the primary pectinate fringe. Thus, some specimens had shorter tergal extensions, without the hair-like distal end, as well as a primary pectinate fringe with barely elongated tips (ca. 20% of the examined specimens) (Fig. 6E). Others had tergal extensions with an elongated, hair-like distal end and primary pectinate fringes with longer tips (ca. 80% of the examined specimens) (Figs. 3A-D; 4E-F; 6F-G). The primary pectinate fringe of segment 10 also showed some intraspecific variation concerning the length of the tips at the ventrolateral region, with ca. 30% of the examined specimens showing conspicuously elongated tips (reaching the edge of segment 11) at this area. Finally, the relative length of the lateral terminal spines also showed intraspecific variability (LTS:TL ratio of 6–10% in 15 out of 52 measured specimens vs. 15–25% in 37 out of 52 measured specimens). These differences were observed in both LM and SEM specimens.

3.1.6 Other remarks

Several specimens (ca. 15% of the total number) had epibionts. The most common ones were filamentous bacteria of different lengths (Figs. 4I; 6G; 8A-C, F-G), but unicellular bacteria were also observed (Fig. 8D-E, H-I). Finally, unknown, rod-shaped epibionts, with a distal constriction, were also detected (Fig. 4H). Epibionts were more commonly found attached to the ventral surface of the posterior segments, the nephridiopore and the lateral terminal spines (Figs. 4H-I; 6G; 8G), but some of them were also present at the anterior segments near sensory spots, tubes, muscular scars and glandular cell outlets (Fig. 8A-F, H-I).

Some specimens (ca. 10% of the total number) had ingested clusters of diatoms at the gut, and even though their frustules seemed to be unaltered, a partially digested, green content was observed (Fig. 4G). This could suggest that the specimens were able to extract the content of the diatom to digest it.

3.2 ***Echinoderes guianensis*** **sp. nov.**

urn:lsid:zoobank.org:act:65E2AD91-5AA4-42D3-A87A-6DE1E56B47DB

(Figs. 9–13, Tables 3–4)

3.2.1 Material examined

Holotype, adult male, collected in November 2017 at the confluence of the Cayenne and Montsinéry Rivers, French Guiana (western Atlantic Ocean): 04°53′49.2288″ N, 52°22′27.714″ W at the intertidal zone in mud; mounted in Fluoromount G®, deposited at MNHN under catalogue number: 664Ma. Paratype, adult female, same collecting data as holotype; mounted in Fluoromount G®, deposited at MNHN under catalogue number: 665Ma. Additional material, one adult male and one adult female, same collecting data as type material; mounted for SEM, stored at IFREMER.

3.2.2 Diagnosis

Echinoderes with short, poorly sclerotized, weakly articulated spines in middorsal position on segment 4, lateroventral position on segment 6 and sublateral position on segment 7, and tubes in lateroventral position on segment 5 and laterodorsal position on segment 10. Enlarged, oval sieve plate in sublateral position on segment 9, consisting of an anterior, slightly convex region with numerous pores and a posterior, slightly concave area with a single, central pore.

3.2.3 Etymology

The specific epithet designates Guiana, the geographical region where the species was found.

3.2.4 Description

See Table 3 for measurements of selected morphological features and body dimensions, and Table 4 for summary of spine, tube, nephridiopore, glandular cell outlet and sensory spot locations.

Ring 00 of mouth cone with nine outer oral styles alternating in size between slightly larger and smaller ones. Outer oral styles composed of two jointed subunits: a rectangular, basal sheath and a triangular, hooked, distally pointed end-piece; basal sheath with a median ridge bearing two short fringes, one basal and another located prior to the junction. Outer oral styles

basally joined by triangular, cuticular thickenings. Outer oral styles located anterior to each introvert sector, except in the middorsal sector 6 where a style is missing (Figs. 9; 12A-B).

Introvert with seven concentric rings of spinoscalids (one ring of primary spinoscalids and six rings or regular-sized spinoscalids) and 10 longitudinal sectors defined by the arrangement of the primary spinoscalids (Fig. 9). Ring 01 with 10 primary spinoscalids, larger than remaining ones, composed of a basal sheath and a distal, elongated, flexible end-piece (Figs. 9; 12C-E). Basal sheath of primary spinoscalids with three overlapping fringes: proximal fringe with three flat projections (trident-like), middle fringe with 7–9 projections becoming shorter towards laterals, distal fringe with 10–12 flat, small, quite inconspicuous projections covering the junction with the end-piece (Fig. 12E). Ring 02 with 10 spinoscalids, arranged as one medially in each sector (Figs. 9; 12C-D). Spinoscalids on this and following rings also composed of a basal sheath and a distal end-piece, smaller than the primary spinoscalids; basal sheath with a proximal, median ridge distally fringed and a distal fringe with 20–25 small projections becoming shorter towards laterals and covering the junction with the end-piece (Fig. 12F). Ring 03 with 20 spinoscalids, arranged as two in each sector. Ring 04 with 10 spinoscalids, arranged as one medially in each sector. Ring 05 with 20 spinoscalids, arranged as two in each sector. Ring 06 with seven spinoscalids, arranged as one medially in each sector except in the sectors 2, 6 and 10. Ring 07 with at least 21 smaller spinoscalids (those of sector 6 not observed) arranged as three in sectors 1, 3 and 9 and two in sectors 2, 4, 5, 7, 8 and 10. Scalid arrangement identical in all sectors from rings 02–05, with one unpaired spinoscalid in ring 02 followed by a quincunx in rings 03–05; in sectors 1, 3 and 9, ring 06 with an unpaired spinoscalid followed by three smaller scalids in ring 07; in sectors 2 and 10, ring 06 without spinoscalids followed by two smaller spinoscalids in ring 07 leaving space for the corresponding trichoscalid and its plate; in sectors 4, 5, 7 and 8, ring 06 with an unpaired spinoscalids followed by two smaller spinoscalids in ring 07 leaving space for the corresponding trichoscalid and its plate (Figs. 9; 12C-D).

Neck with 16 trapezoidal placids, wider at the base, closely adjacent each other, with distinct joint between the neck and first trunk segment. Midventral placid widest (ca. 22µm at base), remaining ones slightly narrower (ca. 13–15µm at base). A ring of six short, superficially haired trichoscalids associated with the placids, attached to mushroom-shaped trichoscalid plates in sectors 2, 4, 5, 7, 8 and 10 (Figs. 9; 10A-B; 11A-B; 121, D, G).

Trunk fusiform, heart-shaped in cross-section, composed of 11 segments. Segments 1–2 closed, ring-like cuticular plates; remaining ones with one tergal and two sternal cuticular

plates; tergosternal junction of segment 3 quite inconspicuous with LM (Figs. 10A-D; 11B; 12A). Maximum sternal width at segment 8, relatively narrow compared to total trunk length (MSW8/TL ratio = 17.2%). Cuticular hairs acicular, non-bracteate, emerging from rounded to slightly oval perforation sites. Cuticular hairs arranged in transversal rows (number of rows increasing towards segment 10) that become wavy at subdorsal and ventrolateral to ventromedial regions, interrupted by large, oval, muscular scars in laterodorsal position where hairs are missing throughout segments 2–10; anterior third of segment 1 without hairs (Figs. 10A-D; 11A-H; 12A; 13A-I). Posterior segment margins straight, with short, finely serrated primary pectinate fringes; tips of primary pectinate fringes conspicuously shorter on segments 4–10 (Figs. 10A-D; 13A-B, D-E, G-H). Secondary pectinate fringes not detected.

Segment 1 with type 1 glandular cell outlet in middorsal and lateroventral positions (Figs. 10A-B; 11A). Rounded sensory spots in subdorsal, laterodorsal and ventromedial positions, the former two near the anterior segment margin, the latter near the posterior segment edge; these sensory spots have 5–6 concentric rings of short micropapillae surrounding one or two central pores (Figs. 10A-B; 11A-B; 13A).

Segment 2 with one pair of droplet-shaped sensory spots in middorsal and ventromedial positions, and two pairs in laterodorsal position (Figs. 10A-B; 11A-B; 13A); on this and following segments, these sensory spots have with numerous, concentric rings of micropapillae surrounding one or two central pores; micropapillae not increasing in length towards the posterior area of the sensory spot (Fig. 13E-I).

Segment 3 with droplet-shaped sensory spots in subdorsal and midlateral positions (Figs. 10B; 11C; 13B).

Segment 4 with spine in middorsal position (Figs. 10B; 11C); spines on this and following segments are acicular, short, poorly sclerotized, weakly articulated, distally frayed (as in Fig. 13D-E). Type 1 glandular cell outlets in subdorsal and ventromedial positions (Figs. 10A-B; 11B).

Segment 5 with tubes in lateroventral position (Figs. 10A; 11D; 13B-C). Type 1 glandular cell outlets in subdorsal and ventromedial positions (Figs. 10A-B; 11D). Droplet-shaped sensory spots in subdorsal, midlateral and ventromedial positions (Figs. 10A-B; 11D; 13B, G).

Segment 6 with spines in lateroventral position (Figs. 10A; 11G; 13B, D). Type 1 glandular cell outlets in subdorsal and ventromedial positions (Figs. 10A-B; 11G). Droplet-shaped sensory spots in subdorsal, midlateral and ventromedial positions (Figs. 10A-B; 11G; 13B, G).

Segment 7 with spines in sublateral position (Figs. 10A; 11H; 13E). Type 1 glandular cell outlets in subdorsal and ventromedial positions (Fig. 10A-B). Droplet-shaped sensory spots in subdorsal, midlateral and ventrolateral positions (Figs. 10A-B; 11H; 13E, H).

Segment 8 with type 1 glandular cell outlets in subdorsal and ventromedial positions (Fig. 10A-B). Droplet-shaped sensory spots in subdorsal position (Fig. 10B).

Segment 9 with type 1 glandular cell outlets in subdorsal and ventromedial positions (Fig. 10A-B). One pair of droplet-shaped sensory spots in midlateral and ventrolateral positions, and two pairs in subdorsal position, mesial ones larger and located more posterior than the lateral ones (Figs. 10A-B; 11E-F; 13F, I). Nephridiopores in sublateral position at the posterior half of the cuticular plate as oval, enlarged sieve plate openings with an anterior, elongated, slightly convex area with numerous pores and a posterior, slightly concave region with a single, central pore (Figs. 10A; 11E; 13I).

Segment 10 with short tubes in laterodorsal position (Fig. 10B, D). Type 1 glandular cell outlets in ventromedial position (Fig. 10A, C). Rounded sensory spots in subdorsal and ventrolateral positions (Fig. 10A-D).

Segment 11 with very short lateral terminal spines (LTS:TL average ratio = 7.6%), distally pointed, with hollow central cavity, covered by hairs throughout the first two thirds (Figs. 10A-D; 12A, H-I). Males with three pairs of penile spines that emerge from laterodorsal position in the intersegmental joint with the preceding segment; penile spines tube-like, abruptly tapering near the distal tips (Figs. 10B; 12I). Females with short lateral terminal accessory spines, covered by hairs, distally pointed (Figs. 10C-D; 12H). Tergal extensions short, triangular, softly rounded at the tips (Figs. 10A-D; 12H-I).

3.2.5 Remarks

One of the examined specimens for SEM had two types of epibionts: unicellular bacteria near the muscular scars of anterior segments and filamentous bacteria of different lengths attached to the segment 11 edge (Fig. 12I).

4. Discussion

4.1 Remarks on diagnostic and differential taxonomic features of Echinoderes angelae *sp. nov. and* E. guianensis *sp. nov., and their assignation to a putative group of* Echinoderes.

The two newly described species have enlarged nephridiopores in sublateral position of segment 9, consisting of an anterior, oval to slightly triangular, convex sieve plate and a posterior, circular to oval, concave region with a single central pore. This feature allows us to include both species in the *Echinoderes coulli*-group. Actually, this character is the only apomorphy of the group, presumably conferring their members a higher osmoregulation efficacy to face salinity fluctuations (Lundbye et al. 2011; Randsø et al. 2019). Other morphological features that also characterize the *E. coulli*-group include poorly developed spines in middorsal position on segment 4 and lateral position on segments 6–7 (if present), poorly developed female lateral terminal accessory spines (if present) and tubes in lateral position on segments 5, 8 and/or 10 (Sørensen 2014; Randsø et al. 2019), features otherwise present in the new species.

Echinoderes angelae sp. nov. possesses spines in middorsal position on segment 4, sublateral position on segments 6–7, tubes in lateroventral position on segments 5, lateral accessory position on segment 8 and laterodorsal position on segment 10. In addition, it has modified type 2 glandular cell outlets in different positions throughout segments 2, 4–8 and 10, and a type of rounded sensory spots on segment 1 characterized by a transversal row of conspicuously elongated hairs at the posterior edge of the papillae area. The spine and tube formula is similar to that of *E. serratulus* Yamasaki, 2016 and *E. cyaneafictus* Cepeda et al., 2022 (Yamasaki 2016; Cepeda et al. 2022) within the *E. coulli*-group. However, *E. cyaneafictus* is easily distinguished from the new species by the absence of type 2 glandular cell outlets (Cepeda et al. 2022). The main morphological difference between *E. serratulus* and *E. angelae* sp. nov. is the presence of midlateral tubes on segment 9 in the former (Yamasaki 2016), which are absent in the latter. Other features that allow their discrimination are the shape of the lateral terminal spines (robust in *E. serratulus* and thin in the new species), the presence of hairs on lateral terminal, lateral terminal accessory and penile spines in *E. angelae* sp. nov. (absent in *E. serratulus*), the absence of cuticular hairs on segment 1 (present in *E. serratulus*), the conspicuous triangular extensions of the posterior midventral edge of segments 2 and 10 in *E. angelae* sp. nov. (not extended in *E. serratulus*) and the arrangement of the type 2 glandular cell outlets (Yamasaki 2016). Type 2 glandular cell outlets are present in the same segments of

both species (except segment 10 that lacks this kind of outlets in *E. serratulus*), but the positions vary from one species to another.

Other *E. coulli*-group congeners with similar arrangement of spines and tubes to *E. angelae* sp. nov. are *E. teretis* Brown, 1999 in Adrianov & Malakhov, 1999 (lateroventral tubes on segment 5, lateroventral spines on segments 6–7, lateral accessory tubes on segment 8), *E. maxwelli* (Omer-Cooper, 1957) (lateroventral tubes on segment 5, lateroventral spines on segment 6, sublateral spines on segment 7, lateral accessory tubes on segment 8), *E. regina* Yamasaki, 2016 (lateroventral tubes on segment 5, sublateral spines on segments 6–7, sublateral tubes on segment 8) and *E. rex* Lundbye et al., 2011 (lateroventral tubes on segment 5, lateroventral spines on segments 6–7, lateroventral tubes on segment 8) (Omer-Cooper 1957; Adrianov & Malakhov 1999; Lundbye et al. 2011; Yamasaki 2016; Randsø et al. 2019). Although these formulas are not the same, identifying the position of spines and tubes in the *E. coulli*-group can be tricky due to the exceptionally small size of these appendages. However, other more obvious characters may be used to distinguish between them. *Echinoderes teretis* lacks lateral terminal accessory spines (Adrianov & Malakhov 1999; Randsø et al. 2019), structures otherwise present in *E. angelae* sp. nov. *Echinoderes maxwelli* possesses a different arrangement of type 2 glandular cell outlets, but the main differences are the presence of type 2 outlets on segment 1 (absent in *E. angelae* sp. nov.) and the absence on segment 10 (present in *E. angelae* sp. nov.) (Randsø et al. 2019). *Echinoderes regina* and *E. rex* are conspicuously larger species (trunk length mean 481µm in *E. regina* and 505 µm in *E. rex* vs. 253µm in *E. angelae* sp. nov.) with, again, a different arrangement of type 2 glandular cell outlets, but the main difference is the absence of these structures on segment 10 (in laterodorsal position on this segment in *E. angelae* sp. nov.) (Lundbye et al. 2011; Yamasaki 2016). In addition, males of *E. rex* possess two pairs of penile spines vs. three pairs in *E. angelae* sp. nov., and females of *E. rex* lack lateral terminal accessory spines, structures otherwise present in *E. angelae* sp. nov. (Lundbye et al. 2011).

Echinoderes guianensis sp. nov. is more distinctive, as its combination of middorsal spine on segment 4 and absence of lateral tubes on segment 8 is unique within the *E. coulli*-group. Actually, the absence of tubes on segment 8 is only shared by some specimens of *E. coulli* Higgins, 1977. The South Carolina population of this species show intraspecific variability regarding this character, which may be present or absent (Higgins 1977; Sørensen, pers. comm.; Yamasaki, pers. comm.). Even in the absence of tubes on segment 8, *E. coulli* differs from the new species in the absence of spines (except for lateral terminal spines).

4.2 Observation of epibiont-basibiont relationships.

Some specimens of *Echinoderes angelae* sp. nov. (ca. 15% of the total number) and *E. guianensis* sp. nov. (ca. 25% of the total number) were found carrying different types of prokaryotic epibionts. Interaction between epibionts and basibionts has been widely studied from an ecological point of view, and may be defined as the attachment of the epibiont to the surface of the basibiont as a support mechanism (Threlkeld et al. 1993; Ansari & Bhadury 2017). Meiofaunal organisms, including nematodes, copepods, ostracods, acari, tanaidaceans and kinorhynchs, may host epibionts (e.g. Dovgal et al. 2008; Souissi et al. 2013; Padmakumar et al. 2015; Chatterjee et al. 2018; Baldrighi et al. 2020). Suctorian and peritrich ciliates, as well as filamentous bacteria, are among the most common epibionts of these meiofaunal groups (e.g. Precht 1935; Schreier & Reysenbach 2019; Chatterjee et al. 2022).

Epibionts are frequently found at the posterior part of the meiofaunal organism bodies, where the anus-cloaca and the gonopores are commonly present (Lynn et al. 2014; Baldrighi et al. 2020). The release of different physiological secretions and excretions (mucus, dregs, excretory fluids, gametes) enhances the attachment of prokaryotic organisms and food particles on the basibiont, and epibionts could profit from this food source (Fernández-Leborans et al. 2017). Indeed, most of the observed kinorhynch specimens had the epibionts attached to the posterior body end (segments 10–11 and lateral terminal spines), near the anus, or in more anterior regions but frequently linked to structures that produce some kind of secretion/excretion, such as the nephridiopore, the tubes, or the glandular outlets. These observations reinforce the hypothesis of epibionts taking advantage of basibionts as attraction of food.

The benefit-cost relationship that the presence of epibionts may cause in the fitness of kinorhynchs is still far from being truly understood. All of the advantages (e.g. camouflage, defense, nutrient acquisition) and disadvantages (e.g. motility reduction, decreased reproduction, resource competition, gas exchange barrier) that have been proposed for other basibionts (Key et al. 1999; Wahl, 2008; Harder, 2009; Fernández-Leborans, 2010; Baldrighi et al. 2020) may apply for Kinorhyncha. Likely, the presence of a few epibionts does not cause a significant decrease of the kinorhynch fitness, but their accumulation could lead to the costs of this ecological interaction outweighing the potential benefits.

4.3 Ecological considerations.

The studied habitat was a low human-impacted mangrove due to the presence of a wastewater treatment plant and some agricultural parcels nearby. Industrial, commercial and urban residuals are drained at the Crique Fouillée tributary. However, none of the potential pollutants present at the area (metals, metalloids, polycyclic aromatic hydrocarbons, polychlorinated biphenyls, pesticides, phthalates, polybromodiphenylethers and alkylphenols) were above the recommended values by the official guideline concentrations for assessing toxicity hazards (Michelet et al. 2021).

Nevertheless, a previous study by Michelet et al. (2021) determined differences in the meiofauna community structure between the three studied stations, partly due to the presence of these contaminants. As suggested by the previous work, an ecological analysis of other meiofaunal groups apart from nematods (including Kinorhyncha) can provide extra information to characterize the quality of the mangrove, which will be left for a future study.

Declaration of competing interest

The authors declare that they have not known competing financial interests or personal relationships that could have appeared to influence the work reported in this paper.

Acknowledgements

French Guiana fieldwork was done by the French working group “Mangroves DCE” under the framework of the European Water Framework Directive (G. Dirberg, C. Hubas, D. Lamy, P. Cuny, C. Militon, R. Walcker, F. Fromard, I. Bihannic, E. Michaud) funded by Office de l’Eau de la Guyane (OEG) and Office Français de la Biodiversité (OFB). The authors are also grateful to LEEISA laboratory (A. Gardel, T. Maury) and IRD for providing laboratory facilities, and to C. Michelet for the meiofauna sorting during her Master’s Internship. Finally, we would like to thank Drs Martin V. Sørensen (Natural History Museum of Denmark) and Hiroshi Yamasaki (Kyushu University) for their useful comments during the review process.

References

Adrianov, A.V., Malakhov, V.V., 1999. Cephalorhyncha of the World Ocean, first ed. KMK Scientific Press, Moscow.

Annapurna, C., Rao, M.S., Bhanu, C.H.V., 2015. Distribution of meiobenthos off Kakinada Bay, Gaderu and Coringa estuarine complex. J. Mar. Biol. Assoc. India 57, 17–26.

Ansari, K.G.M.T., Bhadury, P., 2017. Occurrence of epibionts associated with meiofaunal basibionts from the world's largest mangrove ecosystem, the Sundarbans. Mar. Biodiv. 47, 539–548. https://doi.org/10.1007/s12526-016-0502-5.

Baldrighi, E., Dovgal, I., Zeppilli, D., Abibulaeva, A., Michelet, C., et al., 2020. The cost for biodiversity: records of ciliate-nematode epibiosis with the description of three new suctorian species. Diversity 12, 224. https://doi.org/10.3390/d12060224.

Carus, J.V., 1885. Prodromus Faunae Mediterraneae sive Descriptio Animalium maris Mediterranei incolarum quam comparata silva rerum quatenus innotiut adiectis et nominibus vulgaribus eorumque auctoribus in commodum zoologorum. Vol. I. Coelenterata, Echinodermata, Vermes, Arthropoda, first ed. E. Schweizerbartsche Verlagshandlung E. Koch, Stuttgart.

Castel, J., 1992. The meiobenthos of coastal lagoon ecosystems and their importance in the food web. Vie et Milieu 42, 125–135.

Cepeda, D., González-Casarrubios, A., Sánchez; N., Spedicato, A., Michelet, E., et al., 2022. Two new species of mud dragons (Scalidophora: Kinorhyncha) inhabiting a human-impacted mangrove from Mayotte (Southwestern Indian Ocean). Zool. Anz. 301, 23–41. https://doi.org/10.1016/j.jcz.2022.09.001.

Chatterjee, T., Dovgal, I., Pešić, V., Zawal, A., 2018. A checklist of epibiont suctorian and peritrich ciliates (Ciliophora) on halacarid and hydrachnid mites (Acari: Halacaridae & Hydrachnidia). Zootaxa 4457, 415–430. https://doi.org/10.11646/zootaxa.4457.3.4.

Chatterjee, T., Sautya, S., Dovgal, I., Gaikwad, S., 2022. Report of suctorian ciliates (Ciliophora, Suctorea) as epibionts of meiobenthic nematodes in an oxygen minimum zone of the Arabian Sea, Indian Ocean. Zootaxa 5138, 492–500. https://orcid.org/0000-0001-5532-2726.

Claparède, A.R.É., 1863. Beobachtungen über Anatomie und Entwicklungsgeschichte wirbelloser Thiere: an der Küste von Normandie angestellt, first ed. Verlag von Wilhelm Engelmann, Leipzig.

Della Patrona, L.; Marchand, C.; Hubas, C.; Molnar, N.; Deborde, J.; et al., 2016. Meiofauna distribution in a mangrove forest exposed to shrimp farm effluents (New Caledonia). Mar. Environ. Res. 119, 100–113. https://doi.org/ 10.1016/j.marenvres.2016.05.028.

Dovgal, I., Chatterjee, T., Ingole, B.S., Nanajkar, M., 2008. First report of *Limnoricus ponticus* Dovgal and Lozowskiy (Ciliophora, Suctorea) as epibionts of *Pycnophyes* (Kinorhyncha) from Indian Ocean with key to species of the genus *Limnoricus*. Cah. Biol. Mar. 49, 381–385. https://doi.org/10.21411/CBM.A.4BF662BB.

Edgar G., 1990. The influence of plant structure on the species richness, biomass and secondary production of macrofaunal assemblages associated with Western Australian seagrass beds. J. Exp. Mar. Biol. Ecol. 137, 215–240.

Fernández-Leborans, G., 2010. Epibiosis in Crustacea: an overview. Crustaceana 83, 549–640. https://doi.org/ 10.1163/001121610X491059.

Fernández-Leborans, G., Román, S., Martin, D., 2017. A new deep-sea suctorian-nematode epibiosis (*Loricophyra-Tricoma*) from the Blanes Submarine Canyon (NW Mediterranean). Microb. Ecol. 74, 15–21. https://doi.org/10.1007/s00248-016-0923-5.

Fiard M, Cuny P, Sylvi L, Hubas C, Jézéquel R, et al., 2022. Mangrove microbiota along the urban-to-rural gradient of the Cayenne estuary (French Guiana, South America): Drivers and potential bioindicators. Sci. Tot. Environ. 807, 150667. https://doi.org/10.1016/j.scitotenv.2021.150667.

Gomes C.A.A., Dos Santos, P.J.P., Alves, T.N.C., Rosa-Filho, J.S., Souza-Santos, L.P., 2002. Variaçao temporal da meiofauna em Area de Manguezal em Itamaraca – Pernambuco. Atlântica, Rio Grande 24, 89–96.

Harder, T., 2009. Marine epibiosis: concepts, ecological consequences and host defence. In: Flemming, H.C., Murthy, P.S., Venkatesan, R., Cooksey, K. (Eds.), Marine and Industrial Biofouling, Springer Series on Biofilms. Springer, Berlin, Germany, pp. 219–231. https://doi.org/10.1007/978-3-540-69796-1_12.

Heip, C.H.R., Vincx, M., Vranken, G., 1985. The ecology of marine nematodes. Oceanogr. Mar. Biol. 23, 399–489.

Herranz, M., Stiller, J., Worsaae, K., Sørensen, M.V., 2022. Phylogenomic analyses of mud dragons (Kinorhyncha). Mol. Phylogenet. Evol. 168, 107375. https://doi.org/10.1016/j.ympev.2021.107375.

Higgins, R.P., 1977. Two new species of *Echinoderes* (Kinorhyncha) from South Carolina. Trans. Am. Microsc. Soc. 96, 340–354. https://doi.org/10.2307/3225864.

Hossain, M.D., Nuruddin, A.A., 2016. Soil and mangrove: a review. J. Environ. Sci. Technol. 9, 198–207. https://doi.org/10.3923/jest.2016.198.207.

Kathiresan, K., Bingham, B.L., 2001. Biology of mangroves and mangrove ecosystems. Adv. Mar. Biol. 40, 81–251. https://doi.org/ 10.1016/S0065-2881(01)40003-4.

Key, M.M., Winston, J.E., Volpe, J.W., Jeffries, W.B., Voris, H.K., 1999. Bryozoan fouling of the blue crab *Callinectes sapidus* at Beaufort, North Carolina. Bull. Mar. Sci. 64, 513–533. https://doi.org/10.2307/1549437.

Kirsteuer, E., 1964. Zur Kenntnis der Kinorhynchen Venezuelas. Zool. Anz. 173, 388–393.

Lundbye, H., Rho, H.S., Sørensen, M.V., 2011. *Echinoderes rex* n. sp. (Kinorhyncha: Cyclorhagida), the largest *Echinoderes* species found so far. Sci. Mar. 75, 41–51. https://doi.org/10.3989/scimar.2011.75n1041.

Lynn, D.H., Gómez-Gutiérrez, J., Strüder-Kypke, M., Shaw, C.T., 2014. Ciliate species diversity and host-parasitoid codiversification in the apostome genus *Pseudocollinia* (Ciliophora, Apostomatia, Pseudocollinidae) that infect krill, with description of *Pseudocollinia similis* n. sp., a parasitoid of the krill *Thysanoessa spinifera*. Dis. Aquat. Org. 112, 89–102. https://doi.org/10.3354/dao02796.

Michelet, C., Zeppilli, D., Hubas, C., Baldrighi, E., Cuny, P., et al., 2021. First assessment of the benthic meiofauna sensitivity to low human-impacted mangroves in French Guiana. Forests 12, 338. https://doi.org/10.3390/f12030338.

Mokievsky, V.O., Tchesunov, A.V., Udalov, A.A., Duy-Toan, N., 2011. Quantitative distribution of meiobenthos and the structure of the free-living nematode community of the mangrove intertidal zone in Nha Trang Bay (Vietnam) in the South China Sea. Russ. J. Mar. Biol. 37, 272–283. https://doi.org/10.1134/S1063074011040109.

Olafsson, E., Carlstrom, S., Simon, G.M.N., 2000. Meiobenthos of hypersaline tropical mangrove sediment in relation to spring tide inundation. Hydrobiologia 426, 57–64. https://doi.org/10.1023/A:1003992211656.

Omer-Cooper, J., 1957. Deux nouvelles espèces de Kinorhyncha en Provenance de l'Afrique du Sud. Bull. Mens. Soc. Linn. Lyon 26, 213–216.

Ostmann, O., Nordhaus, I., Sørensen, M.V., 2012. First recording of kinorhynchs from Java, with the description of a new brackish water species from a mangrove-fringed lagoon. Mar. Biodivers. 42, 79–91. https://doi.org/ 10.1007/s12526-011-0094-z.

Padmakumar, K.B., Cicily, L., Vijayan, A.K., Sanjeevan, V.N., 2015. Occurrence of epibiontic suctorian protozoans on marine ostracod *Cypridina dentate* (Muller) in the North Eastern Arabian Sea. Indian J. Mar. Sci. 44, 874–878.

Pillai, N.G., Harilal, C.C., 2018. Mangroves – A review. IJRAMR 5, 4035–4038.

Precht, H., 1935. Epizoen der Kieler Bucht. Nova Acta Leopoldina Halle 3, 405–474.

Randsø, P.V., Yamasaki, H., Bownes, S.J., Herranz, M., Di Domenico, M., et al., 2019. Phylogeny of the *Echinoderes coulli*-group (Kinorhyncha: Cyclorhagida: Echinoderidae) – a cosmopolitan species group trapped in the intertidal. Invertebr. Syst. 33, 501–517. https://doi.org/10.1071/IS18069.

Sahoo, G., Suchiang, S.R., Ansari, Z.A., 2013. Meiofauna-mangrove interaction: a pilot study from a tropical mangrove habitat. Cah. Biol. Mar. 54, 349–358. https://doi.org/10.21411/CBM.A.5CDE9936.

Sasekumar A., Chong V.C., 1998. Faunal diversity in Malaysian mangroves. Glob. Ecol. Biogeogr. Letters 7, 57–60. https://doi.org/ 10.1111/J.1466-8238.1998.00279.X.

Schreier, J.E., Reysenbach, A.L., 2019. Seafloor processes. In: Cochran, J.K., Bokuniewicz, H.J., Yager, P.L. (Eds.), Encyclopedia of Ocean Sciences (3rd Edition). Academic Press, pp. 291–298. https://doi.org/10.1016/B978-0-12-409548-9.11367-3.

Sørensen, M.V., 2014. First account of echinoderid kinorhynchs from Brazil, with the description of three new species. Mar. Biodivers. 44, 251–274. https://doi.org/10.1007/s12526-013-0181-4.

Souissi, A., Souissi, S., Hwang, J.S., 2013. The effect of epibiont ciliates on the behaviour and mating success of the copepod *Eurytemora affinis*. J. Exp. Mar. Biol. Ecol. 445, 38–43. https://doi.org/10.1016/j.jembe.2013.04.002.

Threlkeld, S.T., Chiavelli, D.A., Willey, R.L., 1993. The organization of zooplankton epibionts communities. Trends Ecol. Evol. 8, 317–321. https://doi.org/10.1016/0169-5347(93)90238-K.

Wahl, M., 2008. Ecological lever and interface ecology: epibiosis modulates the interactions between hosts and environment. Biofouling 24, 427–438. https://doi.org/10.1080/08927010802339772.

Yamasaki, H., 2016. Two new *Echinoderes* species (Echinoderidae, Cyclorhagida, Kinorhyncha) from Nha Trang, Vietnam. Zool. Stud. 55, 1–35. https://doi.org/10.6620/ZS.2016.55-32.

Zelinka, C., 1896. Demonstration der Tafeln der *Echinoderes* - Monographie. Verh. Dtsch. Zool. Ges. 6, 197–199.

TABLES.

Table 1. Morphological measurements and dimensions (in µm) of adult specimens of *Echinoderes angelae* sp. nov. from the type locality, including number of measured specimens (*n*), mean value and standard deviation (Sd) of each character, depicted for the holotype and all the measured specimens as a whole. Abbreviations: ac, acicular spine; LD, laterodorsal; LTAS, lateral terminal accessory spine; LTS, lateral terminal spine; LV, lateroventral; MD, middorsal; MSW, maximum sternal width; S, segment length; SL, sublateral; SW, standard sternal width; t, tube; TL, total trunk length; numbers after abbreviations indicate corresponding segment.

Character	Holotype	Range	Mean	Sd, *n*
TL	240	197–319	253	30.7, 52
MSW-8	46	42–61	50	22.9, 37
MSW-8/TL (%)	19	13–23	20	8.8, 37
SW-10	41	26–53	43	19.7, 37
SW-10/TL (%)	17	11–20	17	7.6, 37
S1	29	18–33	25	3.4, 52
S2	24	14–27	22	3.0, 52
S3	22	16–30	22	3.0, 52
S4	28	20–30	24	2.7, 52
S5	26	21–37	27	3.2, 52
S6	31	24–40	30	4.0, 52
S7	36	23–52	34	5.6, 52
S8	45	28–49	39	4.9, 52
S9	46	35–53	43	4.5, 52
S10	42	33–56	43	4.9, 52
S11	28	24–38	31	3.3, 52
MD4 (ac)	8	4–8	6	3.0, 32
LV5 (t)	10	7–12	9	4.6, 29
SL6 (ac)	4	4–6	5	2.4, 18
SL7 (ac)	/	4–7	5	2.8, 27
LV8 (t)	10	7–15	10	5.0, 31
LD10 (t)	13	10–30	20	10.8, 31
LTS	53	21–61	45	15.4, 50
LTS/TL (%)	22	8–28	18	7.2, 50
LTAS	12	12–25	16	7.3, 13
LTAS/LTS (%)	23	21–49	28	13.0, 13

Table 2. Summary of nature and arrangement of acicular spines, tubes, sensory spots, glandular cell outlets, nephridiopores and gonopores in adults of *Echinoderes angelae* sp. nov. Abbreviations: ac, acicular spine; dss, droplet-shaped sensory spot; f, female condition of sexually dimorphic character; gco1, type 1 glandular cell outlet; go, gonopore; LA, lateral accessory; LD, laterodorsal; ltas, lateral terminal accessory spines; lts, lateral terminal spines; LV, lateroventral; m, male condition of sexually dimorphic character; MD, middorsal; mgco2, modified type 2 glandular cell outlet; ML, midlateral; ne, nephridiopore; ps, penile spines; rss, rounded sensory spot; SD, subdorsal; SL, sublateral; t, tube; VL, ventrolateral; VM, ventromedial.

Segment	**MD**	**SD**	**LD**	**ML**	**SL**	**LA**	**LV**	**VL**	**VM**
1	gco1	rss	rss				gco1		rss
2	dss	mgco2	dss, mgco2, dss	mgco2					dss
3	gco1	dss		dss					gco1
4	ac	gco1	mgco2						gco1
5		gco1, mgco2, dss		dss			t		dss, gco1
6		gco1, dss, mgco2		dss, mgco2	ac				dss, gco1
7		gco1, dss, mgco2		dss	ac		mgco2	dss	gco1
8		gco1, mgco2, dss		mgco2		t	mgco2		gco1
9		gco1, dss, dss		dss	ne			dss	gco1
10	gco1, gco1	dss	mgco2, t					dss	gco1
11		dss	ps(m)				lts, ltas(f)	go(f)	dss

Table 3. Morphological measurements and dimensions (in µm) of type material of *Echinoderes guianensis* sp. nov. Abbreviations: ac, acicular spine; LD, laterodorsal; LTAS, lateral terminal accessory spine; LTS, lateral terminal spine; LV, lateroventral; MD, middorsal; ML, midlateral; MSW, maximum sternal width; S, segment length; SW, standard sternal width; t, tube; TL, total trunk length; numbers after abbreviations indicate corresponding segment.

Character	**Holotype (♂) MNHN-664Ma**	**Paratype (♀) MNHN-665Ma**
TL	478	392
MSW-8	82	/
MSW-8/TL (%)	17	/
SW-10	77	/
SW-10/TL (%)	16	/
S1	27	28
S2	24	28
S3	30	29
S4	29	27
S5	40	37
S6	55	42
S7	61	57
S8	70	60
S9	68	67
S10	71	66
S11	42	52
MD4 (ac)	/	/
LV5 (t)	14	9
LV6 (ac)	/	6
ML7 (ac)	6	6
LD10 (t)	/	/
LTS	31	34
LTS/TL (%)	6	9
LTAS	/	/
LTAS/LTS (%)	/	/

Table 4. Summary of nature and arrangement of acicular spines, tubes, sensory spots, glandular cell outlets, nephridiopores and gonopores in adults of *Echinoderes guianensis* sp. nov. Abbreviations: ac, acicular spine; dss, droplet-shaped sensory spot; f, female condition of sexually dimorphic character; gco1, type 1 glandular cell outlet; LD, laterodorsal; ltas, lateral terminal accessory spines; lts, lateral terminal spines; LV, lateroventral; m, male condition of sexually dimorphic character; MD, middorsal; ML, midlateral; ne, nephridiopore; ps, penile spines; rss, rounded sensory spot; SD, subdorsal; SL, sublateral; t, tube; VL, ventrolateral; VM, ventromedial.

Segment	**MD**	**SD**	**LD**	**ML**	**SL**	**LV**	**VL**	**VM**
1	gco1	rss	rss			gco1		rss
2	dss		dss, dss					dss
3		dss		dss				
4	ac	gco1						gco1
5		gco1, dss		dss		t		gco1, dss
6		gco1, dss		dss		ac		gco1, dss
7		gco1, dss		dss	ac		dss	gco1
8		gco1, dss						gco1
9		gco1, dss, dss		dss	ne		dss	gco1
10		rss	t				rss	gco1
11			ps(m)			lts, ltas(f)		

FIGURE CAPTIONS.

Figure 1. Map showing the sampling location in South America (top left), French Guiana (top right) and the Cayenne Estuary (bottom). Sampling stations are marked red circles; mangrove cover is coloured in dark green.

Figure 2. Diagram of mouth cone, introvert and neck placids in *Echinoderes angelae* sp. nov. Grey area and thicker line arcs indicate mouth cone and neck placids, respectively. Spinoscalid positions that are inferred by radial symmetry are marked in grey with dashed line.

Figure 3. Line art drawing of *Echinoderes angelae* sp. nov. A: Ventral female overview; B: dorsal female overview; C: ventral male overview of segments 10–11; D: dorsal male overview of segments 10–11. Abbreviations: dpl, dorsal placid; go, gonopore; lat, lateral accessory tube; lddss, laterodorsal droplet-shaped sensory spot; ldmgco2, laterodorsal modified type 2 glandular cell outlet; ldrss, laterodorsal rounded sensory spot; ldt, laterodorsal tube; ltas, lateral terminal accessory spine; lts, lateral terminal spine; lvgco1, lateroventral type 1 glandular cell outlet; lvmgco2, lateroventral modified type 2 glandular cell outlet; lvt, lateroventral tube; mddss, middorsal droplet-shaped sensory spot; mdgco1, middorsal type 1 glandular cell outlet; mds, middorsal spine; mldss, midlateral droplet-shaped sensory spot; mlmgco2, midlateral modified type 2 glandular cell outlet; ms, muscular scar; mvpl, midventral placid; ppf, primary pectinate fringe; ps, penile spines; S, segment (followed by number of corresponding segment); sddss, subdorsal droplet-shaped sensory spot; sdgco1, subdorsal type 1 glandular cell outlet; sdmgco2, subdorsal modified type 2 glandular cell outlet; sdrss, subdorsal rounded sensory spot; slne, sublateral nephridiopore; sls, sublateral spine; te, tergal extension; tsp, trichoscalid plate; vldss, ventrolateral droplet-shaped sensory spot; vmdss, ventromedial droplet-shaped sensory spot; vmgco1, ventromedial type 1 glandular cell outlet; vmrss, ventromedial rounded sensory spot.

Figure 4. Light micrographs of female holotype MNHN-655Ma (A, C-D), male paratype MNHN-661Ma (B, E), female paratypes MNHN-656Ma (H) and MNHN-657Ma (F), and additional specimens (G, I) of *Echinoderes angelae* sp. nov. showing trunk overview, details of mouth cone and neck, epibionts and ingested diatoms. A: Ventral trunk overview; B: mouth cone, showing the outer oral styles; C: dorsal neck view; D: ventral neck view; E: middorsal to laterodorsal view on right side of tergal plate of segments 10–11; F: lateral view of segment 11; G: ingested diatom; H: unknown type of epibionts attached to the posterior edge of segment 11; I: filamentous bacteria attached to the posterior edge of segment 11. Abbreviations: ba, bacteria;

bs, basal sheath; dpl, dorsal placid; ep, end-piece; ldt, laterodorsal tube; ltas, lateral terminal accessory spine; lts, lateral terminal spine; mvpl, midventral placid; ps, penile spines; te, tergal extension; tsp, trichoscalid plate.

Figure 5. Light micrographs of female holotype MNHN-655Ma (E), male paratype MNHN-661Ma (C-D), and additional specimens (A-B, F) of *Echinoderes angelae* sp. nov. showing trunk cuticular details. A: Middorsal to midlateral view on right side of tergal plate of segments 1–2; B: midlateral to ventromedial view on left side of cuticular plates of segments 5–7; C: ventral view of segments 5–6; D: dorsal view of segments 8–9; E: midlateral to ventromedial view on right side of cuticular plates of segments 9–10 (inset shows the intraspecific variability of the nephridiopore); F: midlateral to ventromedial view on right side of cuticular plates of segments 7–8. Abbreviations: lat, lateral accessory tube; lvt, lateroventral tube; ms, muscular scar; ppf, primary pectinate fringe; slne, sublateral nephridiopore; sls, sublateral spine; numbers after abbreviation indicate corresponding segment; glandular cell outlets are marked with continuous circles, and sensory spots with dashed circles or teardrop-like figures.

Figure 6. Scanning electron micrographs of additional specimens of *Echinoderes angelae* sp. nov. showing trunk overview and details of introvert, neck, lateral terminal spines and sexually dimorphic features. A: Lateral trunk overview; B: introvert, sector 3; C: introvert, sector 4; D: ventral neck view; E: lateral terminal spine; F: male penile spines; G: female lateral terminal accessory spine. Abbreviations: ba, bacteria; ftz, fringed transverse zone; ltas, lateral terminal accessory spine; lts, lateral terminal spine; mvpl, midventral placid; ne, neck; ps, penile spines; psp, primary spinoscalid; sp, spinoscalid (followed by number of corresponding ring); te, tergal extension; ts, trichoscalid; tsp, trichoscalid plate; lambda marks (^) indicate attachment point of spinoscalids.

Figure 7. Scanning electron micrographs of additional specimens of *Echinoderes angelae* sp. nov. showing trunk segments and details of cuticular appendages. A: Subdorsal and laterodorsal sensory spots of segment 1, with the enlarged external ring of micropapillar (inset shows the intraspecific variability of these structures without such kind of external ring); B: ventral view of segments 2–6; C: subdorsal (top) and laterodorsal (bottom) modified type 2 glandular cell outlets of segments 2 and 4 respectively; D: laterodorsal view on left side of tergal plate of segment 2; E: nephridiopore and midlateral droplet-shaped sensory spot of segment 9; F: subdorsal to midlateral view on right side of tergal plates of segments 8–9; G: middorsal spine of segment 4; H: subdorsal to midlateral view on left side of tergal plates of segments 3–4; I: laterodorsal tube of segment 10; J: lateral accessory tube of segment 8 (left) and sublateral spine

of segment 7 (right); K: subdorsal type 1 glandular cell outlet of segment 9; L: ventral view of segments 10–11; M: subdorsal droplet-shaped sensory spot of segment 9. Abbreviations: go, gonopore; ms, muscular scar; spf, secondary pectinate fringe; modified type 2 glandular cell outlets are marked with continuous circles, and sensory spots with dashed teardrop-like figures.

Figure 8. Scanning electron micrographs showing two types of prokaryotic (likely bacteria) epibionts found on additional specimens of *Echinoderes angelae* sp. nov. A: Sternal plates of segments 6–7 with filamentous bacteria; B: sternal plates of segments 6–8 with filamentous bacteria; C: filamentous bacteria attached to the ventromedial droplet-shaped sensory spot of segment 6; D: bacteria near the ventrolateral droplet-shaped sensory spot of segment 2; E: bacteria on the muscular scar of segment 6; F: filamentous bacteria attached to the subdorsal enlarged sensory spot of segment 1; G: sternal plates of segments 9–11 and lateral terminal spines with filamentous bacteria; H: bacteria near the lateroventral tube of segment 5; I: bacteria and filamentous bacteria on nephridiopore of segment 9. Abbreviations: tu, tube; arrows indicate the presence and/or attachment point of bacteria and filamentous bacteria respectively.

Figure 9. Diagram of mouth cone, introvert and neck placids in *Echinoderes guianensis* sp. nov. Grey area and thicker line arcs indicate mouth cone and neck placids, respectively. Spinoscalids that may be absent in some sectors are marked in grey with dashed line.

Figure 10. Line art drawing of *Echinoderes guianensis* sp. nov. A: Ventral male overview; B: dorsal male overview; C: ventral female overview of segments 10–11; D: ventral female overview of segments 10–11. Abbreviations: dpl, dorsal placid; lddss, laterodorsal droplet-shaped sensory spot; ldrss, laterodorsal rounded sensory spot; ldt, laterodorsal tube; ltas, lateral terminal accessory spine; lts, lateral terminal spine; lvgco1, lateroventral type 1 glandular cell outlet; lvs, lateroventral spine; lvt, lateroventral tube; mddss, middorsal droplet-shaped sensory spot; mdgco1, middorsal type 1 glandular cell outlet; mds, middorsal spine; mldss, midlateral droplet-shaped sensory spot; ms, muscular scar; mvpl, midventral placid; ppf, primary pectinate fringe; ps, penile spines; S, segment (followed by number of corresponding segment); sddss, subdorsal droplet-shaped sensory spot; sdgco1, subdorsal type 1 glandular cell outlet; slne, sublateral nephridiopore; sls, sublateral spine; te, tergal extension; tsp, trichoscalid plate; vmdss, ventromedial droplet-shaped sensory spot; vmgco1, ventromedial type 1 glandular cell outlet; vmrss, ventromedial rounded sensory spot.

Figure 11. Light micrographs of male holotype MNHN-664Ma (B-H) and female paratype MNHN-665Ma (A) of *Echinoderes guianensis* sp. nov. showing trunk cuticular details. A:

Middorsal to midlateral view on right side of tergal plates of segments 1–2; B: ventral view of segments 1–4; C: middorsal to laterodorsal view on right side of tergal plates of segments 3–4; D: midlateral to ventromedial view on left side of cuticular plates of segment 5; E: detail of the nephridiopore of segment 9; F: middorsal to laterodorsal view on left side of tergal plate of segment 9; G: midlateral to ventromedial view on left side of cuticular plates of segment 6; H: detail of the midlateral spine of segment 7. Abbreviations: dpl, dorsal placid; lvs, lateroventral spine; lvt, lateroventral tube; mds, middorsal spine; mvpl, midventral placid; sls, sublateral spine; tsp, trichoscalid plate. glandular cell outlets are marked with continuous circles, and sensory spots with dashed circles or teardrop-shaped figures.

Figure 12. Scanning electron micrographs of additional specimens of *Echinoderes guianensis* sp. nov. showing trunk ventral overview and details of mouth cone, introvert, neck, lateral terminal spines and sexually dimorphic features. A: Ventral trunk overview; B: mouth cone outer oral styles; C: introvert, sector 1; D: introvert, sector 4; E: detail of primary spinoscalids; F: detail of regular-sized spinoscalids; G: detail of trichoscalid; H: detail of lateral terminal accessory and lateral terminal spines; I: detail of penile spines. Abbreviations: ba, bacteria; bs, basal sheath; ct, cuticular thickening; ep, end-piece; fr, fringe (preceded by corresponding number of fringe); in, introvert; ltas, lateral terminal accessory spine; lts, lateral terminal spine; mc, mouth cone; ne, neck; ps, penile spine; psp, primary spinoscalid; ts, trichoscalid; lambda marks (^) indicate attachment point of spinoscalids.

Figure 13. Scanning electron micrographs of additional specimens of *Echinoderes guianensis* sp. nov. showing trunk segments and details of cuticular appendages. A: Ventrolateral to ventromedial view of cuticular plates of segments 1–2; B: lateral view of segments 3–6; C: lateroventral tube of segment 5; D: lateroventral spine of segment 6; E: sublateral spine and droplet-shaped sensory spot of segment 7; F: subdorsal droplet-shaped sensory spots of segment 9; G: right sternal plates of segments 5–6; H: right sternal plates of segments 7–8; I: midlateral droplet-shaped sensory spot and sublateral nephridiopore of segment 9. Abbreviations: lvt, lateroventral tube; lvs, lateroventral spine; ms, muscular scar; droplet-shaped sensory spots are marked with teardrop-like figures.

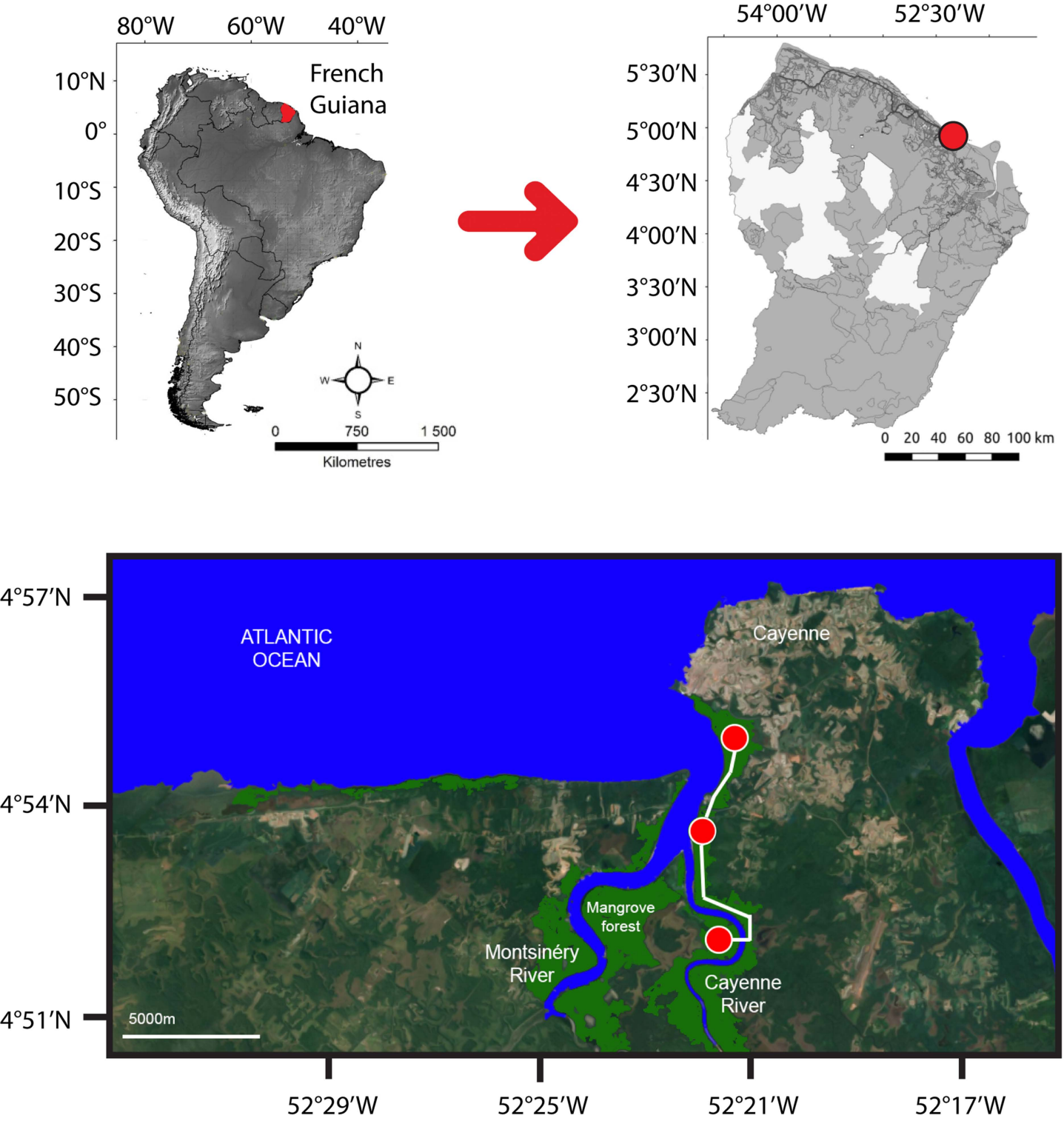
80°W
60°W
40°W
10°N
0°
10°S
20°S
30°S
40°S
50°S
French
Guiana
N
W
E
S
0
750
1 500
Kilometres
54°00′W
52°30′W
5°30′N
5°00′N
4°30′N
4°00′N
3°30′N
3°00′N
2°30′N
0 20 40 60 80 100 km
4°57′N
4°54′N
4°51′N
ATLANTIC
OCEAN
Cayenne
Mangrove
forest
Montsinéry
River
Cayenne
River
5000m
52°29′W
52°25′W
52°21′W
52°17′W

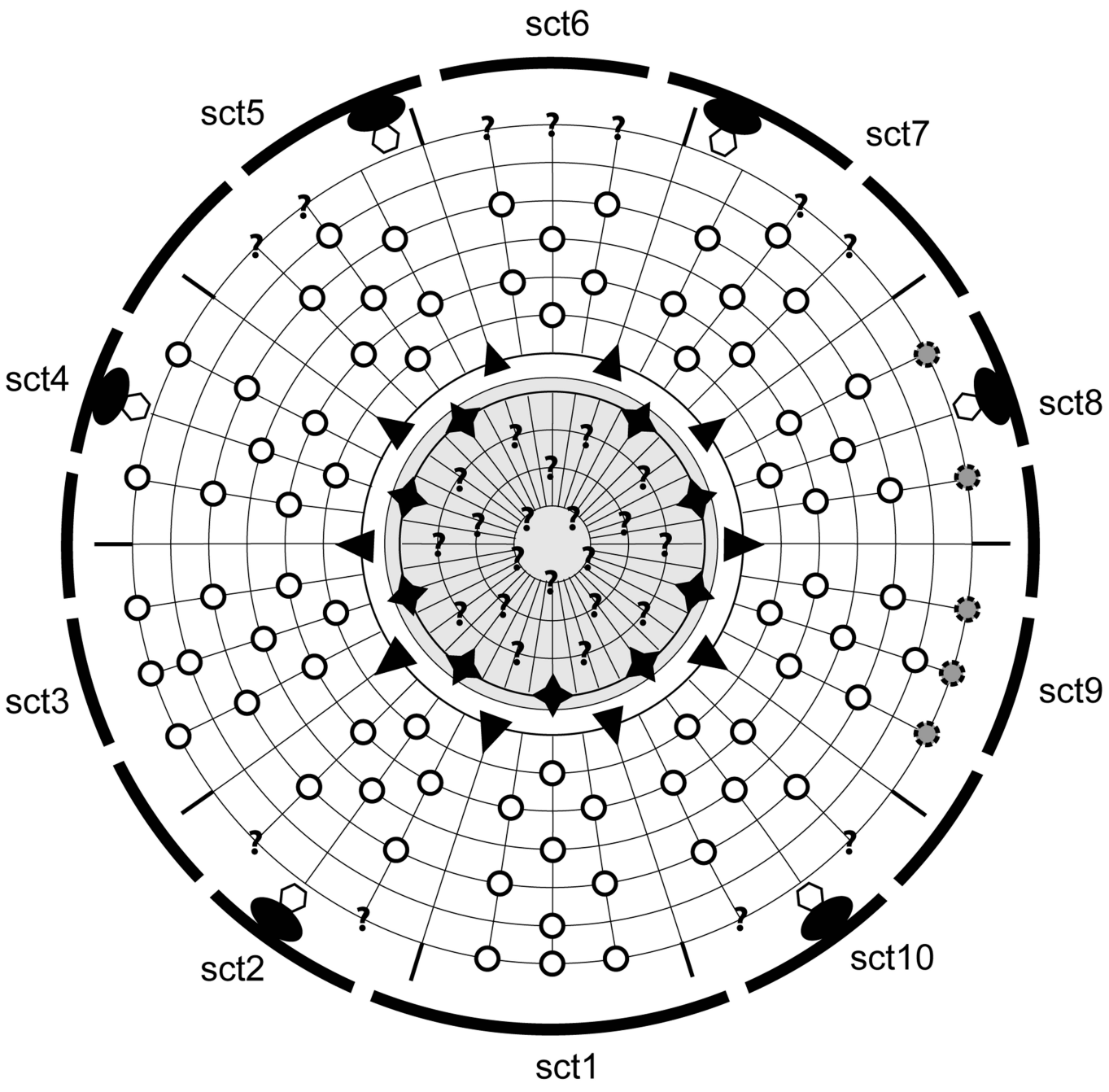

Scalid and style arrangement

By ring:

Ring -03: ? helioscalids
Ring -02: ? inner oral styles
Ring -01: ? inner oral styles
Ring 00: 9 outer oral styles
Ring 01: 10 spinoscalids
Ring 02: 10 scalids
Ring 03: 20 scalids
Ring 04: 10 scalids
Ring 05: 20 scalids
Ring 06: 5 scalids
Ring 07: at least 10 scalids
Trichoscalid row: 6 trichoscalids

By sector:

Odd sectors: 7/10 scalids

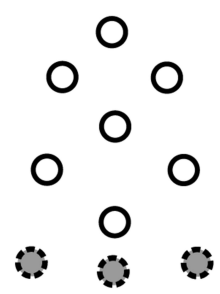

Even sectors: 6/8 scalids

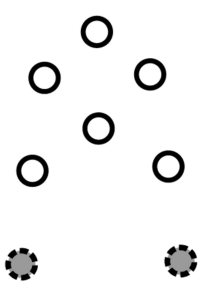

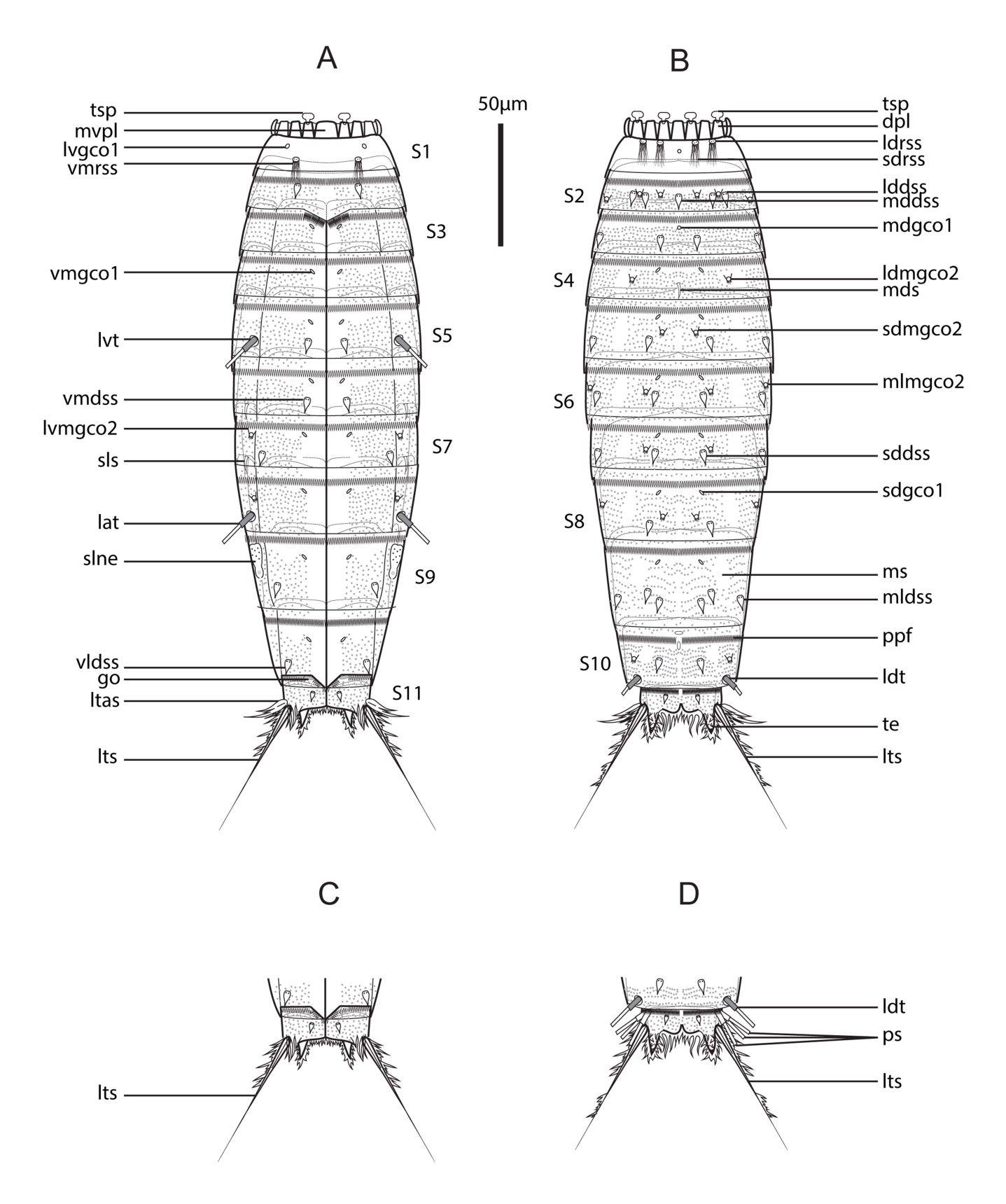
A
B
C
D
50µm
tsp
mvpl
lvgco1
vmrss
vmgco1
lvt
vmdss
lvmgco2
sls
lat
slne
vldss
go
ltas
lts
S1
S3
S5
S7
S9
S11
tsp
dpl
ldrss
sdrss
lddss
mddss
mdgco1
ldmgco2
mds
sdmgco2
mlmgco2
sddss
sdgco1
ms
mldss
ppf
ldt
te
lts
S2
S4
S6
S8
S10
lts
ldt
ps
lts

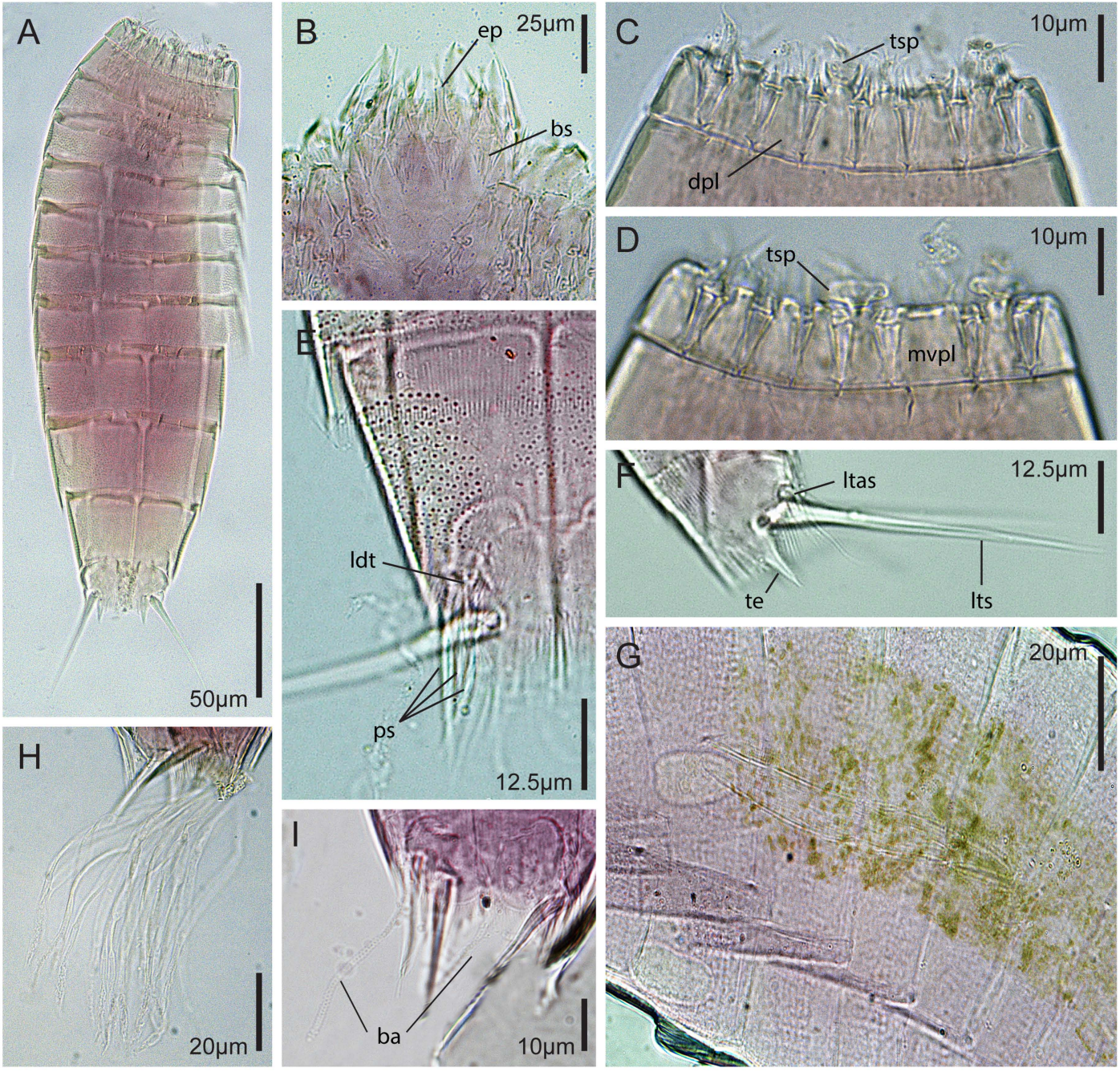
A
50µm
B
ep
25µm
bs
C
tsp
10µm
dpl
D
tsp
10µm
mvpl
E
ldt
ps
12.5µm
F
ltas
12.5µm
te
lts
G
20µm
H
20µm
I
ba
10µm

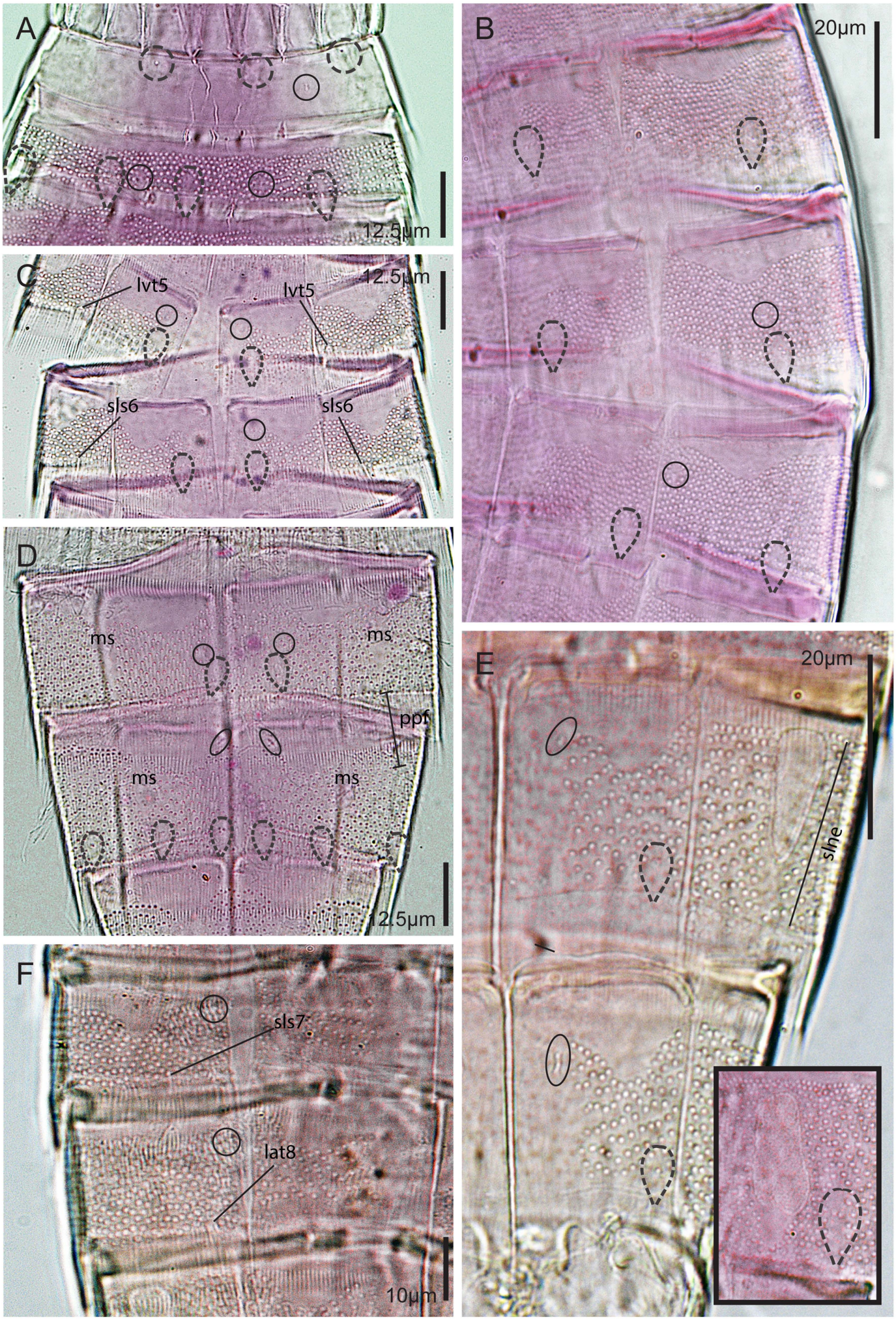
A
12.5µm
B
20µm
C
lvt5
lvt5
12.5µm
sls6
sls6
D
ms
ms
ppf
ms
ms
12.5µm
E
20µm
slne
F
sls7
lat8
10µm

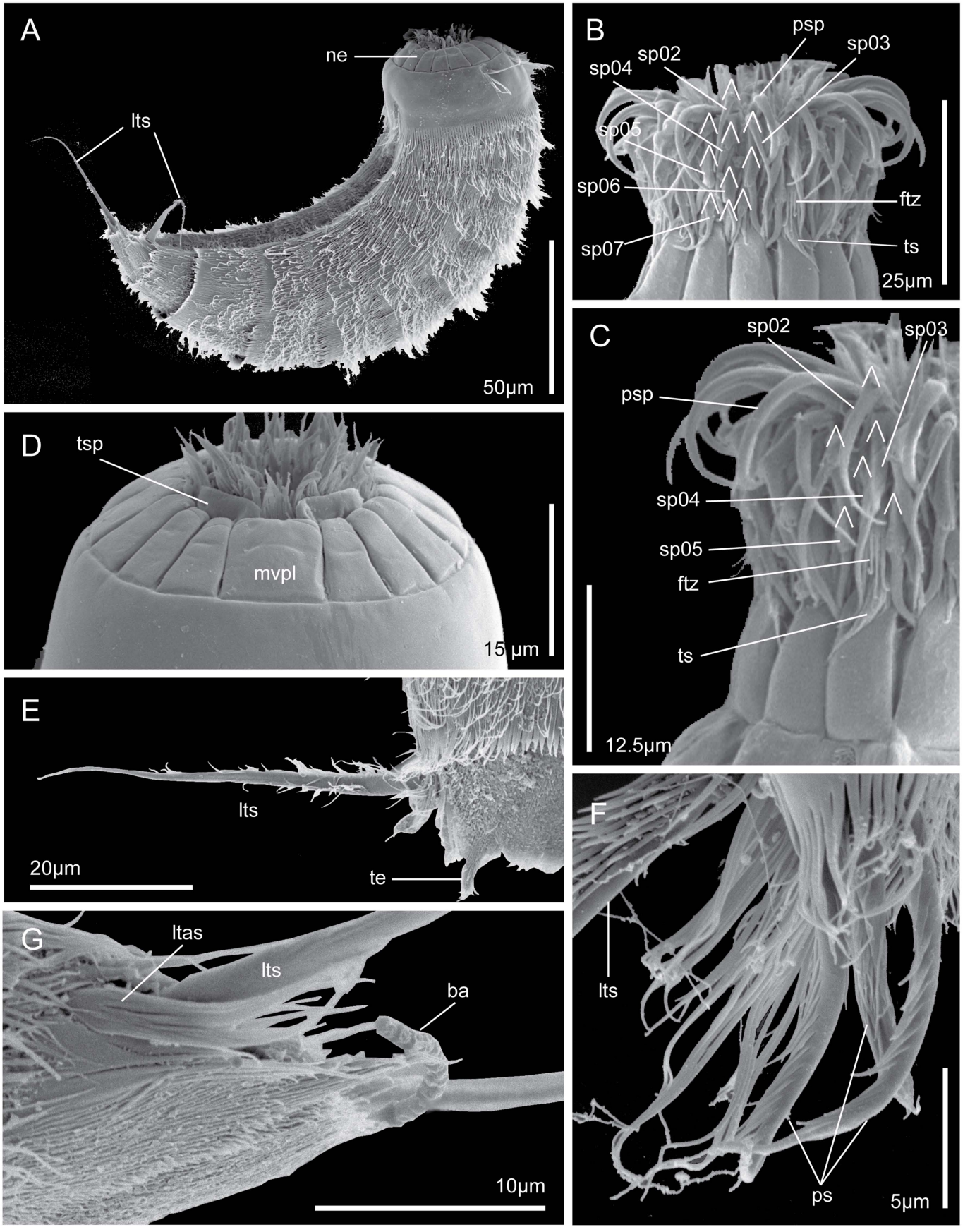
A
ne
lts
50µm
B
psp
sp03
sp02
sp04
sp05
sp06
sp07
ftz
ts
25µm
C
sp02
sp03
psp
sp04
sp05
ftz
ts
12.5µm
D
tsp
mvpl
15 µm
E
lts
20µm
te
F
lts
ps
5µm
G
ltas
lts
ba
10µm

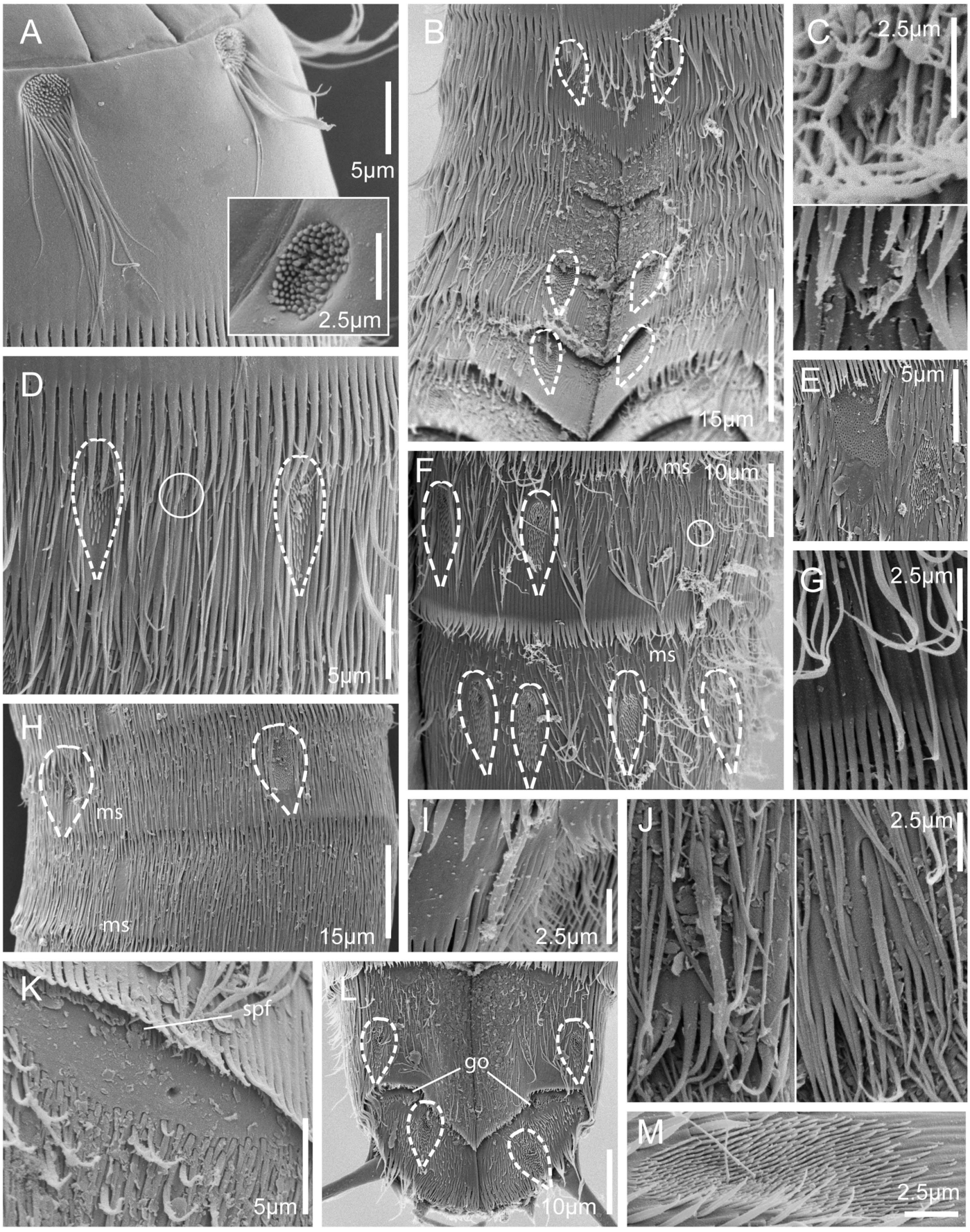
A
5µm
2.5µm
B
15µm
C
2.5µm
D
5µm
E
5µm
F
ms
10µm
ms
G
2.5µm
H
ms
ms
15µm
I
2.5µm
J
2.5µm
K
spf
5µm
L
go
10µm
M
2.5µm

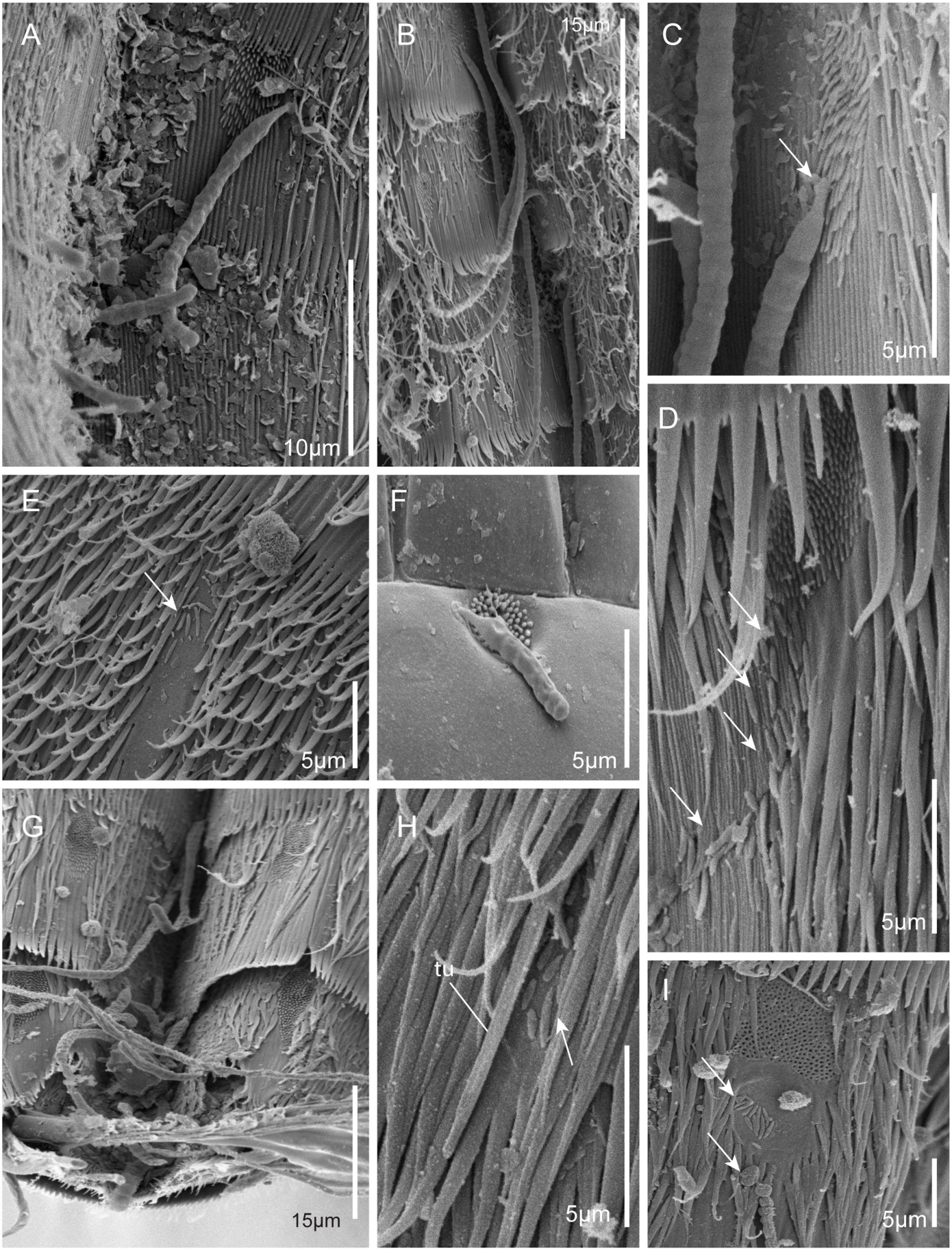
A
10μm
B
15μm
C
5μm
D
5μm
E
5μm
F
5μm
G
15μm
H
tu
5μm
I
5μm

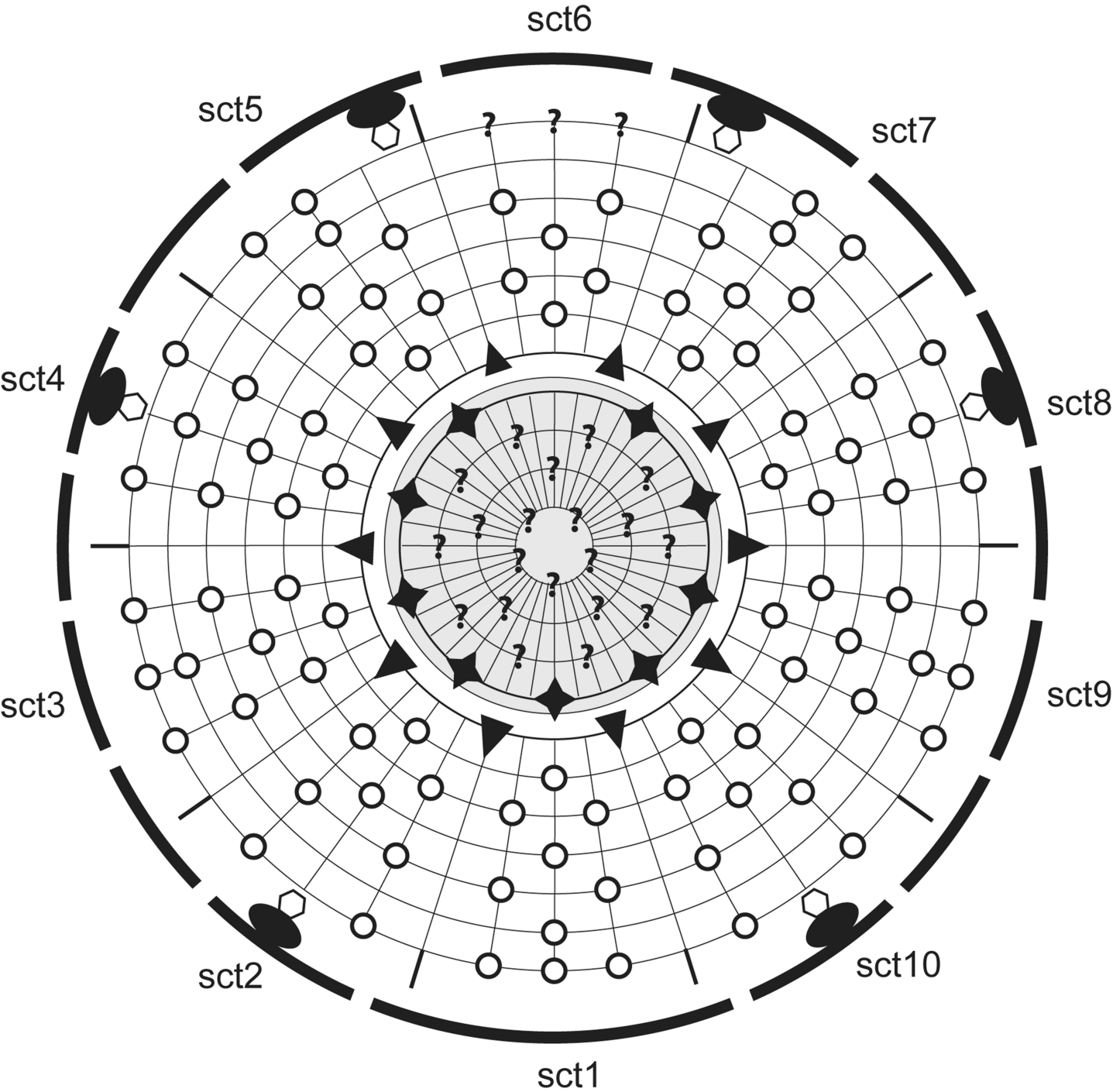

Scalid and style arrangement

By ring:

Ring -03: ? helioscalids
Ring -02: ? inner oral styles
Ring -01: ? inner oral styles
Ring 00: 9 outer oral styles
Ring 01: 10 spinoscalids
Ring 02: 10 scalids
Ring 03: 20 scalids
Ring 04: 10 scalids
Ring 05: 20 scalids
Ring 06: 7 scalids
Ring 07: at least 21 scalids
Trichoscalid row: 6 trichoscalids

By sector:

Odd sectors: 9/10 scalids

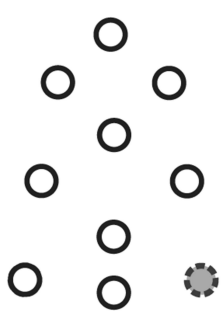

Even sectors: 8/9 scalids

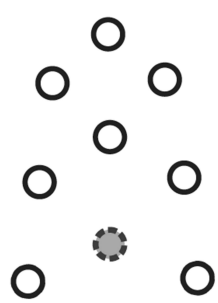

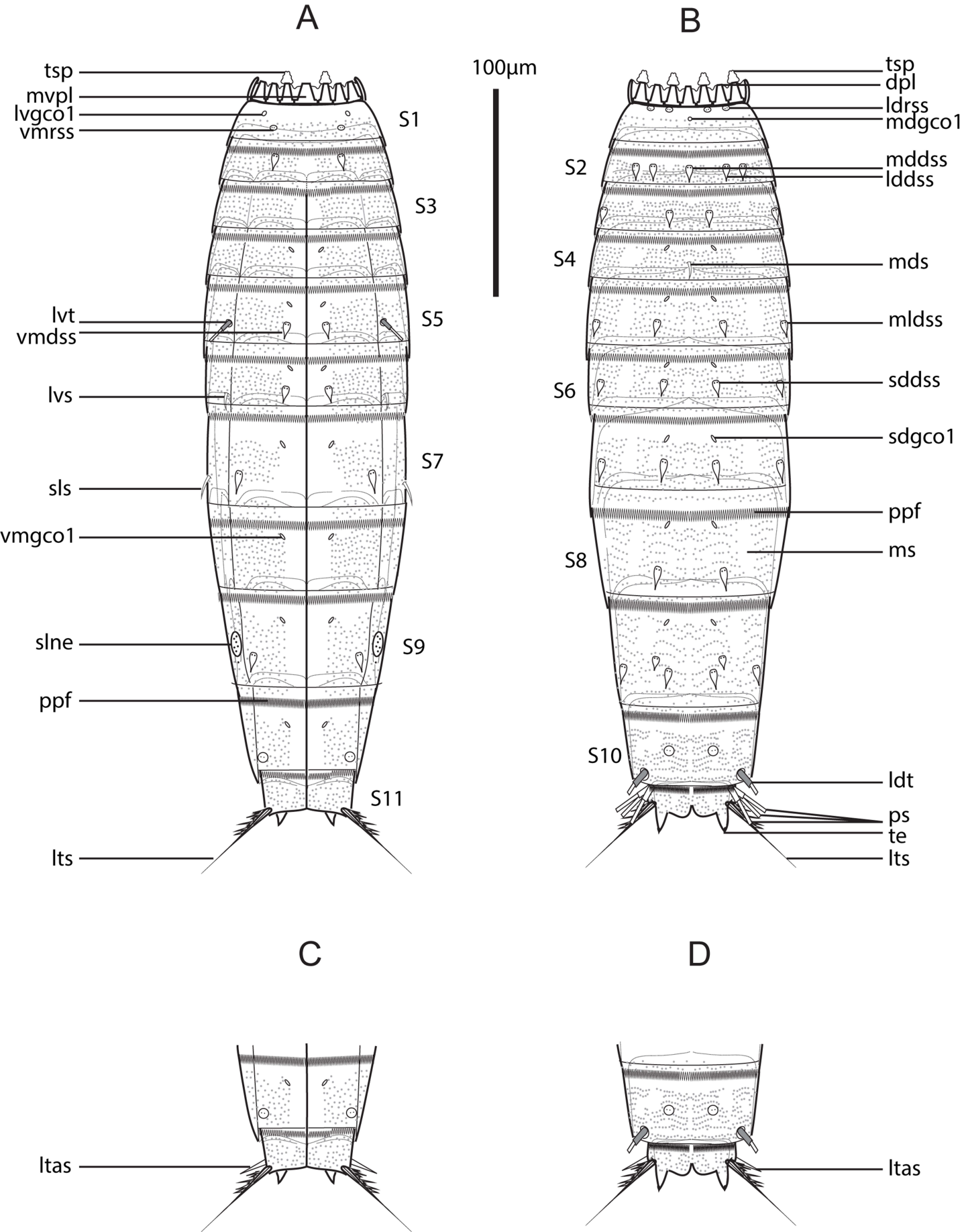
A
B
C
D
100µm
tsp
mvpl
lvgco1
vmrss
S1
S3
lvt
vmdss
S5
lvs
S7
sls
vmgco1
slne
S9
ppf
S11
lts
tsp
dpl
ldrss
mdgco1
S2
mddss
lddss
S4
mds
mldss
S6
sddss
sdgco1
ppf
ms
S8
S10
ldt
ps
te
lts
ltas
ltas

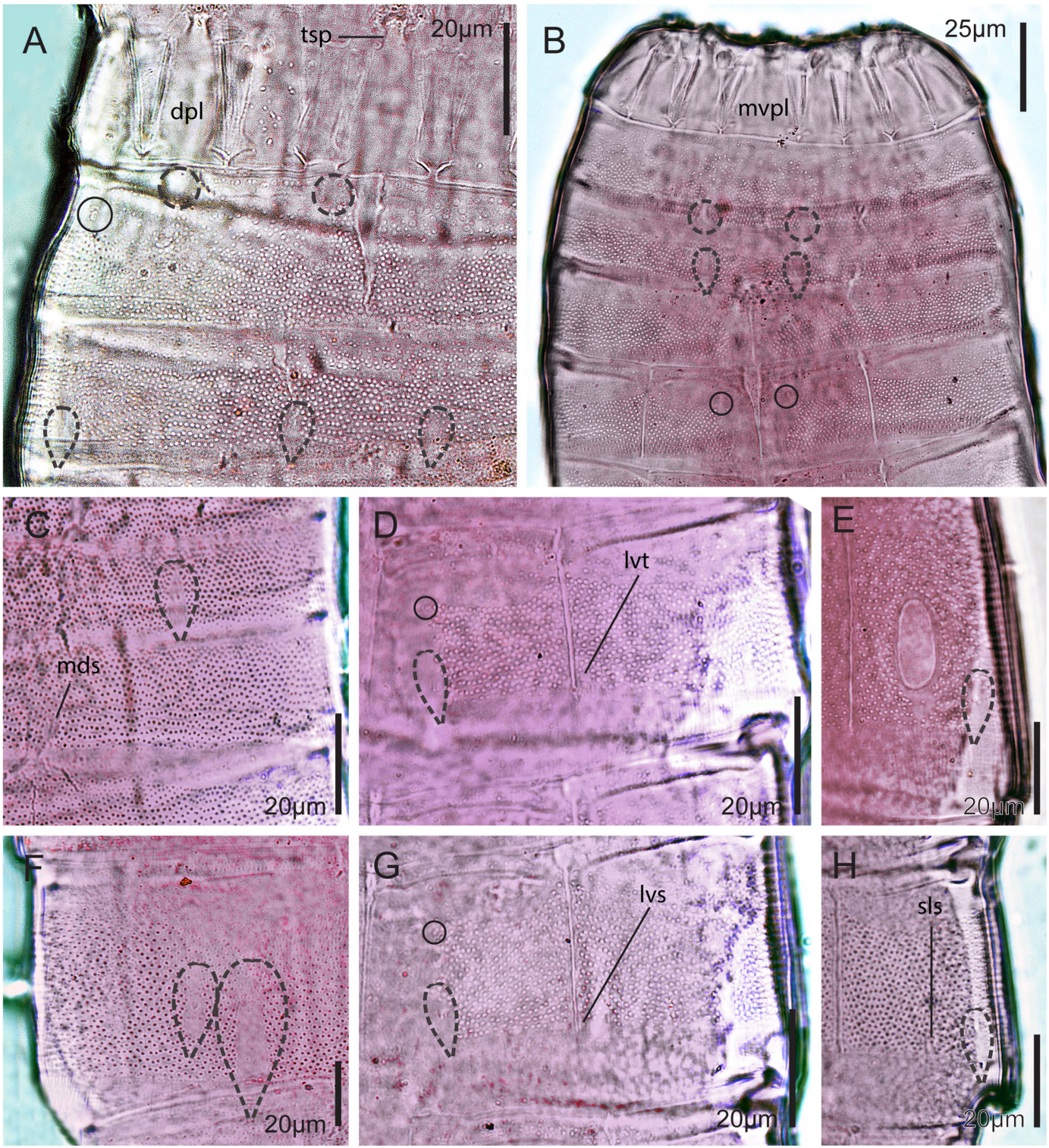
A
tsp
20µm
dpl
B
25µm
mvpl
C
mds
20µm
D
lvt
20µm
E
20µm
F
20µm
G
lvs
20µm
H
sls
20µm

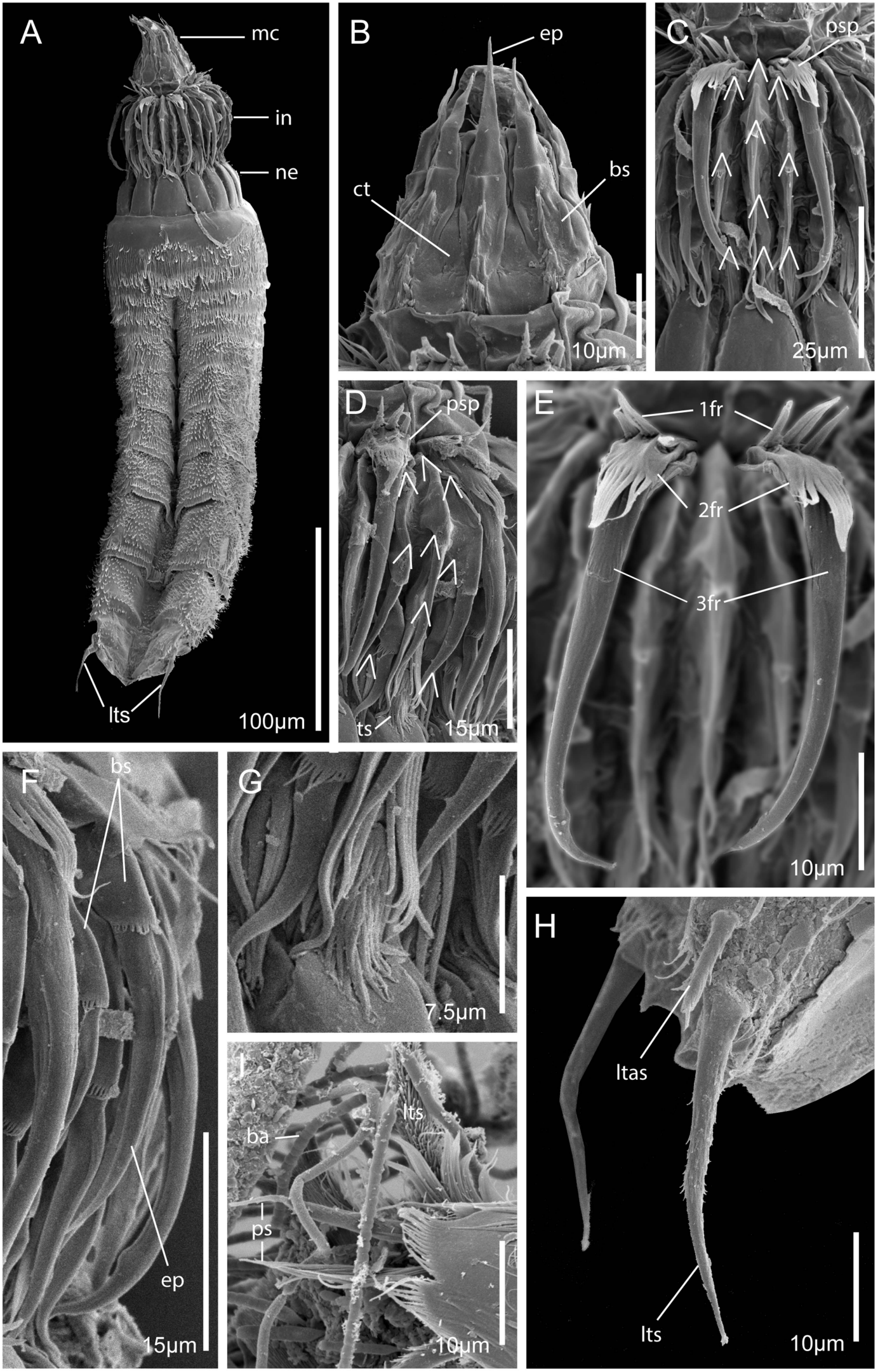
A
mc
in
ne
lts
100µm
B
ep
bs
ct
10µm
C
psp
25µm
D
psp
ts
15µm
E
1fr
2fr
3fr
10µm
F
bs
ep
15µm
G
7.5µm
J
lts
ba
ps
10µm
H
ltas
lts
10µm

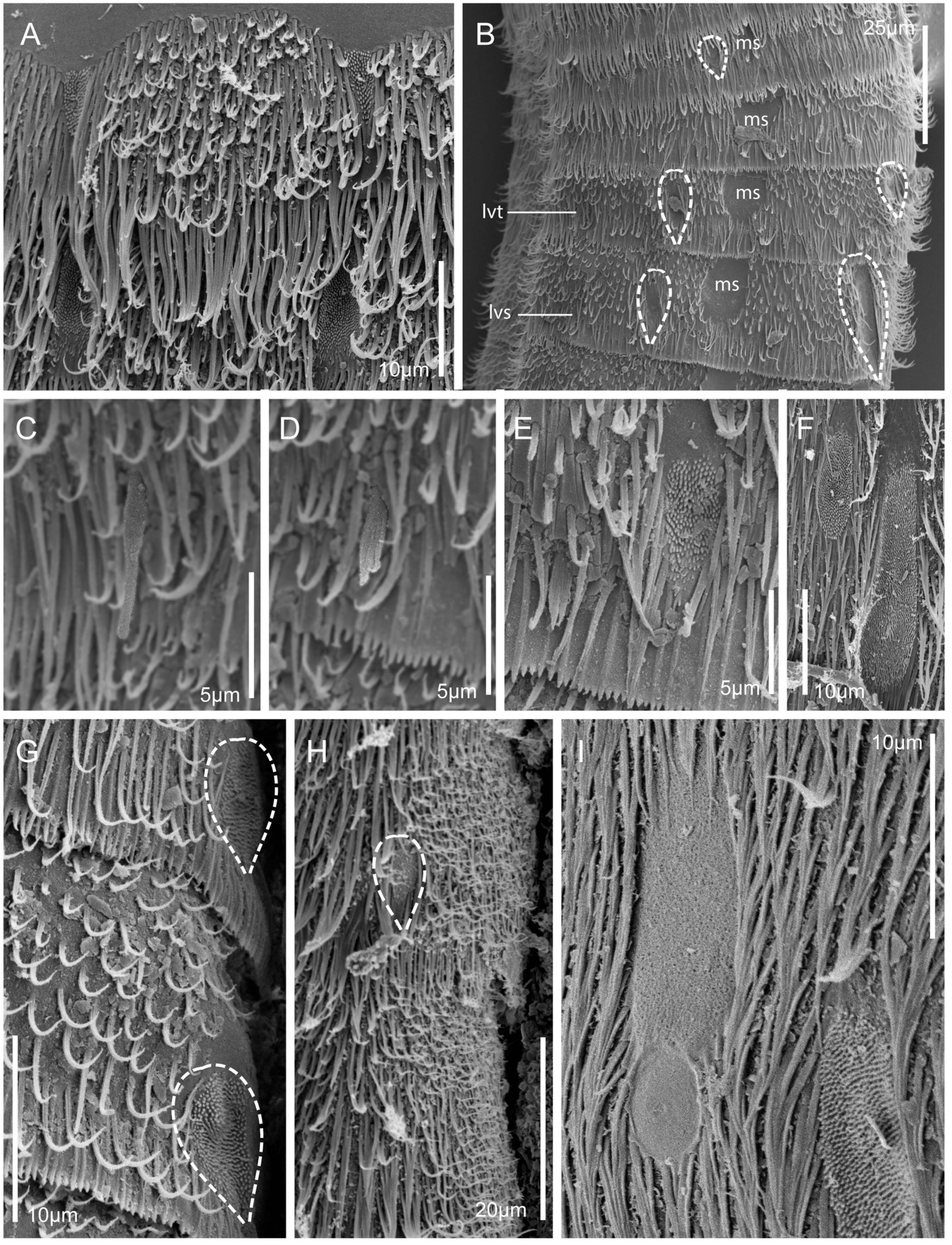
A
10µm
B
25µm
ms
ms
ms
ms
lvt
lvs
C
5µm
D
5µm
E
5µm
F
10µm
G
10µm
H
20µm
I
10µm

Declaration of interests

☒ The authors declare that they have no known competing financial interests or personal relationships that could have appeared to influence the work reported in this paper.

☐ The authors declare the following financial interests/personal relationships which may be considered as potential competing interests: